NOAA Technical Memorandum NOS OR&R 43

ALOHA®
(AREAL LOCATIONS OF HAZARDOUS ATMOSPHERES) 5.4.4

TECHNICAL DOCUMENTATION

Seattle, Washington
November 2013

DEPARTMENT OF COMMERCE • National Oceanic and Atmospheric Administration (NOAA)
National Ocean Service • Office of Response and Restoration

NOAA's Office of Response and Restoration

NOAA's Office of Response and Restoration (OR&R) is a center of expertise in preparing for, evaluating, and responding to threats to coastal environments, including oil and chemical spills, releases from hazardous waste sites, and marine debris.

To fulfill its mission of protecting and restoring NOAA trust resources, the Office of Response and Restoration:

- Provides scientific and technical support to prepare for and respond to oil and chemical releases.
- Determines damage to natural resources from these releases.
- Protects and restores marine and coastal ecosystems, including coral reefs.
- Works with communities to address critical local and regional coastal challenges.

OR&R is comprised of three divisions: Emergency Response, Assessment and Restoration, and Marine Debris. Collectively, the Office of Response and Restoration provides comprehensive solutions to environmental hazards caused by oil, chemicals, and marine debris.

For comments, questions, or copies of this document, please contact: ORR.CAMEO@NOAA.GOV

Cite as:
Jones, R., W. Lehr, D. Simecek-Beatty, R. Michael Reynolds. 2013. ALOHA® (Areal Locations of Hazardous Atmospheres) 5.4.4: Technical Documentation. U. S. Dept. of Commerce, NOAA Technical Memorandum NOS OR&R 43. Seattle, WA: Emergency Response Division, NOAA. 96 pp.

NOAA Technical Memorandum NOS OR&R 43

ALOHA® (Areal Locations of Hazardous Atmospheres) 5.4.4
Technical Documentation

Robert Jones,[1] William Lehr,[1] Debra Simecek-Beatty,[1] R. Michael Reynolds[2]

[1] National Oceanic and Atmospheric Administration
Office of Response and Restoration
Emergency Response Division
7600 Sand Point Way
Seattle, WA 98115

[2] National Oceanic and Atmospheric Administration (retired)

November 2013
Seattle, WA

U.S. DEPARTMENT OF COMMERCE
Penny Pritzker
Secretary

National Oceanic and Atmospheric Administration
Kathryn D. Sullivan, Ph.D.
Acting Under Secretary of Commerce for Oceans and Atmosphere, and Acting Administrator

National Ocean Service
Holly A. Bamford, Ph.D.
Assistant Administrator for Ocean Services and Coastal Zone Management

DEPARTMENT OF COMMERCE
National Oceanic and Atmospheric Administration
National Ocean Service
Office of Response and Restoration
Emergency Response Division
Seattle, Washington, United States of America

TABLE OF CONTENTS

Frequently-used Symbols

g	acceleration of gravity (9.8 m s^{-2})
Pr	Prandtl number
R	gas constant (8.314 J mol^{-1} K^{-1})
Re	Reynolds number
Sc	Schmidt number
Sc_T	Turbulent Schmidt number
T	Temperature (K)
t	time (s)
x	position in downwind direction (m)
y	position in horizontal crosswind direction (m)
z	position in vertical direction (m)
U	wind speed (m s^{-1})

EXECUTIVE SUMMARY

A description of the conceptual and mathematical models that form the basis of the ALOHA computer application are described. ALOHA is designed for use during accidental chemical spills to help spill response professionals assess the risk to human populations associated with toxic air hazards, thermal radiation from fires, and blast effects.

ALOHA is designed to provide a close upper bound to the threat distances associated with chemical spills of a scale typical of transportation accidents, with typical threat zones in the range of 100 to 10,000 meters. ALOHA is limited to hazards associated with chemical vapors or chemicals that become airborne. ALOHA includes an extensive library of chemical property data, and models to assess the rate at which a chemical is released from containment and vaporizes. ALOHA links source strength models to air dispersion models to estimate the spatial extent of airborne hazards.

ALOHA uses a graphical interface for data entry, and display of results. Exposures to toxic chemical vapors, overpressure, thermal radiation, or areas where flammable gases are present are represented graphically and with a text summary.

1 INTRODUCTION

1.1 ABOUT ALOHA

ALOHA is a stand-alone software application developed for the Windows and Macintosh operating systems. It was developed and is supported by the Emergency Response Division[1] (ERD), a division within the National Oceanic and Atmospheric Administration (NOAA) in collaboration with the Office of Emergency Management of the Environmental Protection Agency (EPA). Its primary purpose is to provide emergency response personnel estimates of the spatial extent of some common hazards associated with chemical spills. The ALOHA development team also recognizes that ALOHA can be an appropriate tool for training and contingency planning, but users should remain aware of its primary purpose in spill response. ALOHA provides estimates of the spatial extent of some of the hazards associated with the short-term accidental release of volatile and flammable chemicals. ALOHA deals specifically with human health hazards associated with inhalation of toxic chemical vapors, thermal radiation from chemical fires, and the effects of the pressure wave from vapor-cloud explosions.

Since ALOHA is limited to chemicals that become airborne, it includes models to assess the rate at which a chemical is released from containment and vaporizes. These "source strength" models can be critical components in the process of assessing hazards. ALOHA links source strength models to a dispersion model to estimate the spatial extent of toxic clouds, flammable vapors, and explosive vapor clouds. However, ALOHA does not model all combinations of source strength, scenario, and hazard category for combustion scenarios. The user must choose a specific combination from a limited selection. Table 1 shows the combination of source strength models, scenarios, and hazard categories allowed in ALOHA.

ALOHA uses a graphical interface for data entry and display of results. The area where there is a possibility of exposure to toxic vapors, a flammable atmosphere, overpressure from a vapor cloud explosion, or thermal radiation from a fire are represented graphically as threat zones. Threat zones represent the area within which the ground-level exposure exceeds the user-specified level of concern at some time after the beginning of a release. All points within the threat zone experience a transient exposure exceeding the level of concern at some time following the release; it is a record of the predicted peak exposure over time. In some scenarios, the user can also view the time dependence of the exposure at specified points.

[1] The Emergency Response Division (ERD), formerly Hazardous Materials Response Division (HAZMAT), supports emergency response and restoration activities for oil and hazardous chemical spills, provides preparedness aids for response communities, and offers training on the scientific aspects of oil and chemical spill response.

Table 1. Hazard categories modeled in ALOHA.

Scenario\Source	*Direct source*	*Tank*	*Puddle*	*Gas Pipeline*
Vapor cloud	Toxic vapors	Toxic vapors	Toxic vapors	Toxic vapors
Vapor cloud (flash fire)	Flammable area	Flammable area	Flammable area	Flammable area
Vapor cloud (explosion)	Overpressure	Overpressure	Overpressure	Overpressure
Pool fire	NA	Thermal radiation	Thermal radiation	NA
BLEVE (fireball)	NA	Thermal radiation	NA	NA
Jet fire	NA	Thermal radiation	NA	Thermal radiation

1.2 DESIGN CRITERIA AND LIMITATIONS

To achieve ALOHA's function as a tool for emergency response, the following design criteria were given priority:

ALOHA was designed to provide an assessment of threat zones using information that is commonly available to responders during an emergency. The user is required to provide data on local atmospheric conditions, the identity of the chemical, and details about the spill scenario. To minimize input data requirements, an extensive database of chemical properties and geographical data are included in ALOHA.

ALOHA is designed to provide a close upper bound to the threat distances associated with chemical spills. Wherever uncertainty is unavoidable, ALOHA will err in favor of overestimating rather than underestimating threat distances. In some cases, ALOHA will significantly overestimate threat zones.

ALOHA was designed to be easy to use so that responders can use it during a spill event. ALOHA's user interface is designed to minimize operator error. Navigation through the model input screens is designed to be intuitive and quick. User input data is checked for consistency and reasonableness. Results are presented graphically.

ALOHA provides methods for estimating the release and volatilization rate of chemicals for many common accident scenarios.

ALOHA runs quickly on small computers (PC or Macintosh) that are easily transportable and affordable for most users.

ALOHA is designed to predict hazards associated with spills of a scale that are typical of transportation accidents. Typical scales for threat zones are in the range of 10^2 to 10^5 meters, with durations of up to an hour.

ALOHA is limited in its ability to account for the effects associated with terrain and buildings. ALOHA uses a wind field that does not vary with time or horizontal position, but does vary with elevation. As such, it cannot resolve the steering effects from features in the terrain or buildings. ALOHA is applicable to cases where the wind speed is greater than 1 meter per second (at 10 meters); it should not be used for very low wind speeds or calm conditions.

1.3 ABOUT THIS DOCUMENT

ALOHA includes data compilations, source strength models, and models to estimate hazard associated with airborne chemicals. This document describes the theoretical basis for these models, but does not describe the computer algorithms used to solve the associated numerical problems. It is organized into 6 chapters, each corresponding to a set of related functions performed by ALOHA.

Chapter 2 describes the databases contained within ALOHA. ALOHA includes physical, chemical, and toxicological properties for over 500 pure chemicals and some common chemical solutions. ALOHA also includes latitudes, longitudes, altitudes, and time zone data for many cities in the USA.

Chapter 3 encompasses the source strength models used to estimate the amount of material becoming airborne, thereby contributing to an airborne toxic or flammable cloud. ALOHA includes models that estimate the rate at which a chemical is released from a tank or gas pipeline, or evaporates from a puddle. In addition, the user can directly specify the amount of chemical entering the atmosphere.

Chapter 4 describes the air dispersion models that are at the core of ALOHA's methodology for estimating the inhalation hazard associated with toxic airborne chemicals, and the extent of a flammable cloud. These air dispersion models are used to predict how the concentration of a pollutant, once released into the air, varies with time and position. ALOHA incorporates two semi-empirical air dispersion models: the Gaussian model is used to predict the wind-dominated transport of pollutant clouds that are not significantly affected by gravity; the Heavy Gas model is used for pollutant clouds that are significantly affected by gravity due to their densities.

Chapter 5 deals with the models employed to estimate the effects associated with a vapor cloud explosion. In rare events, volatile chemicals released into the air have formed clouds with proper ratios of fuel to air, ignited, and burned sufficiently quickly to produce damaging shockwaves. The speed at which the combustion progresses through the cloud determines whether the combustion of a vapor cloud produces a shock wave with damaging overpressures extending beyond the bounds of the fire. ALOHA integrates air dispersion models and vapor cloud explosion models to estimate the extent of an area affected by a damaging overpressure.

Chapter 6 describes the models used to estimate the thermal radiation hazard associated with fires. Fires of sufficient size and duration can produce intense thermal radiation that poses a threat to human health and safety far beyond the bounds of the fire. Many chemicals found in the ALOHA database can be ignited and sustain a combustion when mixed with air. ALOHA can estimate the thermal radiation from pool fires, jet fires, and fireballs associated with BLEVEs. The user can view the peak thermal energy flux from a combustion process or thermal energy flux as a function of time. The threat zone associated with flash fires is also described in this chapter, but the thermal

radiation associated with flash fires is not explicitly modeled. ALOHA computes the area within which the chemical vapors might exceed the lower flammability limits.

2 THE INTEGRAL DATABASES

ALOHA includes data files with physical, chemical, and toxicological properties for hundreds of pure chemicals and some common chemical solutions. The chemical data files include chemicals that have the potential to be involved in accidental releases and generate toxic air hazards or pose the threat of fire or explosion. The chemicals included in the ALOHA chemical library are a subset of those found in CAMEO CHEMICALS, a database of hazardous chemicals compiled and maintained by the Emergency Response Division of NOAA and the Office of Emergency Management in EPA (see http://cameochemicals.noaa.gov/).

2.1 TOXICOLOGICAL DATA

ALOHA employs Levels of Concern (LOC) to address the impact of toxic air plumes, fires, and explosions on human populations. For inhalation hazards, ALOHA's LOCs are concentrations of airborne chemicals associated with adverse health effects. Since ALOHA is used primarily for situations where the goal is to assess the threat posed to the general public by a chemical release, it includes LOCs that are specifically designed to predict how the general public will respond to a short-term release. In limited cases, exposure guidelines developed for worker safety are also compiled and presented to users as an option.

LOCs for toxic inhalation hazards are specific to the chemicals. Thresholds for inhalation toxicity are extracted from CAMEO Chemicals. AEGLs (Acute Exposure Guideline Levels), ERPGs (Emergency Response Planning Guidelines), PACs (Protective Action Criteria), and IDLH (Immediate Danger to Life and Health) limits are stored within data files integrated into ALOHA.

AEGLs, ERPGs, and PACs, are tiered public exposure guidelines developed for accidental chemical release events. (See http://orise.orau.gov/emi/scapa/ for a more complete description.) Though developed by different organizations, all three exposure guidelines share a similar approach in appraising the effects of chemical exposure in their use of levels to describe the increasing severity associated with increasing concentration. In addition, these exposure levels are differentiated by exposure times. AEGLs have been developed for a range of exposure times; ALOHA only includes 60-minute AEGLs. ERPGs are defined for 60-minute exposures.

IDLH (Immediate Danger to Life and Health) limits (Barsan, United States. Dept. of Health and Human Services., and National Institute for Occupational Safety and Health. 2010) are included in the list of LOCs available to users. They were developed primarily for making decisions regarding respirator use. In the 1980s, before public exposure guidelines were available for most common chemicals, the IDLH limit was used in public exposure situations. Unlike the three-tiered public exposure guidelines, only a single IDLH value is defined for applicable chemicals.

2.2 FLAMMABILITY

ALOHA includes data on chemical flammability. The lower flammability and upper flammability limits are included in the chemical library. These data were extracted from DIPPR (American Institute of Chemical Engineers).

2.3 PHYSICAL PROPERTIES

A chemical name, CAS registry number, molecular weight, and toxicological data are included for every chemical in the data file. These are the minimum data required for the Direct Source option and the Gaussian dispersion model in ALOHA.

The other options in ALOHA, such as Source Strength modeling, Heavy Gas modeling, and modeling for fires and explosions require more extensive datasets. Full datasets are available for about half the chemicals in the data file; the additional physical property data required were extracted from the DIPPR data compilation, a proprietary database containing physical constants and formulas for temperature dependent properties (American Institute of Chemical Engineers). Data are available for the following properties: critical temperature, critical pressure, critical volume, freezing point, normal boiling point, vapor pressure, liquid density, gas density, heat of vaporization, heat of combustion, liquid heat capacity, and vapor heat capacity.

Data required to model the evaporation of solutions is stored in a separate data file. ALOHA allows the user to model solutions within limited concentration ranges. In most cases, the upper limit is determined by the concentration range that is commonly available for shipment commercially. The lower limit was set such that the expected downwind air plume would be below toxic levels; the lower limit is often the concentration of the azeotropic mixture. Partial pressure, liquid density, liquid heat capacity, and heat of vaporization are functions of both temperature and concentration. Tabulated partial pressure data for a range of concentration and temperature are stored in a data file; ALOHA interpolates between data points using a linear interpolation in log(Pressure) and (1/Temperature). Formulas for liquid density (kg/m^3), liquid heat capacity (J/kg K), and heat of vaporization (J/kg) were developed by fitting tabulated data to a polynomial equation of the form

$$Value = C_1 + C_2 \times Temperature + C_3 \times MassFraction + C_4 \times \left(MassFraction\right)^2 .$$

Hydrochloric acid solutions with concentrations between 20% by mass and 42% by mass can be modeled in ALOHA. Vapor pressure tables were extracted from Perry's Chemical Engineer's Handbook, 6th edition (Perry, Green, and Maloney 1984). The coefficients for the heat capacity and density formulas were based on a least squares polynomial fit to data found in Perry's Chemical Engineer's Handbook, 6th edition (Perry, Green, and Maloney 1984). The coefficients for the heat of vaporization were derived from heat of formation data found in the NBS Technical Note 270-1 (Wagman and Rossini 1965).

Table 2. Coefficients for polynomials describing physical properties of hydrochloric acid.

	C_1	C_2	C_3	C_4
Density (kg/m³)	1152.8	-0.5	502.0	0
Heat capacity (J/kg K)	2470.8	4.0	-3390.8	0
Heat of vaporization (J/kg)	2023600	0	-476800	-1776900

Ammonia solutions with concentrations less or equal to 30% by mass can be modeled in ALOHA. Vapor pressure tables were extracted from Perry's Chemical Engineer's Handbook, 6th edition (Perry, Green, and Maloney 1984). The coefficients for the heat capacity and density formulae were based on a least squares polynomial fit to data found in Perry's Chemical Engineer's Handbook, 6th edition (Perry, Green, and Maloney 1984). The coefficients for the heat of vaporization were derived from heat of formation data found in the NBS Technical Note 270-1 (Wagman and Rossini 1965).

Table 3. Coefficients for polynomials describing physical properties of ammonia solutions.

	C_1	C_2	C_3	C_4
Density (kg/m³)	1101.7	-0.4	-315.4	0
Heat capacity (J/kg K)	2625.8	5.3	-26.9	0
Heat of vaporization (J/kg)	2003900	0	-241700	-715500

Nitric acid solutions with concentrations between 69% by mass and 100% by mass can be modeled in ALOHA. Vapor pressure tables were extracted from Perry's Chemical Engineer's Handbook, 6th edition (Perry, Green, and Maloney 1984). The coefficients for the heat capacity formulae were based on a polynomial fit to the data found in the Kirk-Othmer Encyclopedia of Chemical Technology, 4th edition (Kirk et al. 1991). The coefficients for the density formulae were based on a least squares polynomial fit to data found in Perry's Chemical Engineer's Handbook, 6th edition (Perry, Green, and Maloney 1984). The coefficients for the heat of vaporization were derived from heat of formation data found in the NBS Technical Note 270-1 (Wagman and Rossini 1965).

Table 4. Coefficients for polynomials describing physical properties of nitric acid.

	C_1	C_2	C_3	C_4
Density (kg/m3)	1672	-1.7	331.2	0
Heat capacity (J/kg K)	4016	0	-2260	0
Heat of vaporization (J/kg)	1181100	0	-41300	-520200

Hydrofluoric acid solutions with concentrations between 37% by mass and 70% by mass can be modeled in ALOHA. Though solutions with concentrations exceeding 70% are commercially available, ALOHA does not model these due to the complexity of the chemistry. Vapor pressure tables were extracted from Kirk-Othmer Encyclopedia of Chemical Technology, 3rd edition (Kirk et al. 1978). The coefficients for the heat capacity formulas were based on a linear fit to data in the Kirk-Othmer Encyclopedia of Chemical Technology, 4th edition (Kirk et al. 1991). The coefficients for the density formulas were based on a least squares polynomial fit to data found in Perry's Chemical Engineer's Handbook, 6th edition (Perry, Green, and Maloney 1984). The coefficients for the heat of vaporization were derived from heat of formation data found in the NBS Technical Note 270-1 (Wagman and Rossini 1965).

Table 5. Coefficients for polynomials describing physical properties of hydrofluoric acid.

	C_1	C_2	C_3	C_4
Density (kg/m³)	477.5	1.67	609.3	-296.0
Heat capacity (J/kg K)	4148	0	-1942.6	0
Heat of vaporization (J/kg)	2424600	0	-324200	0

Oleum is a mixture of sulfur trioxide and anhydrous sulfuric acid. Mixtures with concentrations of free sulfur trioxide between 4% by weight and 65% by weight can be modeled in ALOHA.

Coefficients for the density formula were based on 3 values, 20%, 25%, and 30%, reported in the Enviro TIPS manual (Environmental Protection Service. 1984) and a graph in Ullmann's Encyclopedia of Industrial Chemistry (Ullmann 2000) which showed the dependence on temperature. Coefficients for the heat capacity formula were based on a graph in the Kirk-Othmer Encyclopedia of Chemical Technology, 4th edition (Kirk et al. 1991). Heat of Vaporization is an average of the values presented by Brand and Rutherford (Brand and Rutherford 1952); there appears to be no discernible dependence on concentration. The Vapor pressures for up to 34% can be found in Brand and Rutherford, and are complemented by measurement by Schrage (Schrage 1991).

Table 6. Coefficients for polynomials describing physical properties of oleum.

	C_1	C_2	C_3	C_4
Density (kg/m³)	2162	-1.1	360	0
Heat capacity (J/kg K)	1333	0	485.7	0
Heat of vaporization (J/kg)	712756	0	0	0

2.4 WARNINGS

In addition to data required to model release and downwind dispersion, ALOHA also includes data used to trigger warning statements while running the model. One option in ALOHA allows the user to model releases on water. Since ALOHA does not have the methods for modeling soluble chemical spills on water, the user is given a warning that the chemical is soluble. Information about which chemicals in ALOHA have solubilities exceeding 50 kg/m^3 was based on data extracted from the CHEMWATCH database (Chemwatch).

Some chemicals are sufficiently reactive that they undergo chemical reactions when in contact with air or moisture. The ALOHA development team examined every chemical in ALOHA to determine which would likely react sufficiently to have significant impacts on the accuracy of the dispersion models. Information about these reactive chemicals is included in a data file.

2.5 GEOGRAPHICAL DATA

ALOHA includes latitudes, longitudes, altitudes, and time zone data for many cities in the USA. These data are used to compute solar radiation and local ambient pressure.

3 SOURCE STRENGTH MODELS

3.1 BACKGROUND

The rate at which a chemical becomes airborne is critical to the size and duration of a toxic or flammable cloud. ALOHA employs a variety of models to estimate the rate at which a chemical is released from confinement and enters the atmosphere; these are referred to as source strength models. ALOHA can predict source strength for four general classes of chemical releases, or sources:

- Direct. An instantaneous or continuous release of chemical vapors into the air from a single point. This is the only option that allows for an elevated release.
- Puddle. A puddle of constant area, containing either a non-boiling or boiling liquid.
- Tank. A cylindrical or a spherical tank at ground level with a single hole or leaking valve. The tank may contain a liquid, pressurized gas, or gas liquefied under pressure. Tank contents may escape directly into the atmosphere or first form a spreading evaporating pool.
- Gas pipeline. A pressurized pipe containing gas, either connected to a very large reservoir or unconnected to any storage vessel.

ALOHA limits the duration of any source to one hour, and the shortest source duration allowed in ALOHA is one minute (this is termed an instantaneous release in ALOHA). In most cases, source strength changes continuously over the duration of the release. ALOHA approximates continuously variable releases with a series of very short steady-state releases. Up to 150 time-steps are used to model time-varying releases. These timesteps are reduced to five or fewer steady-state timesteps which are linked to the dispersion models.

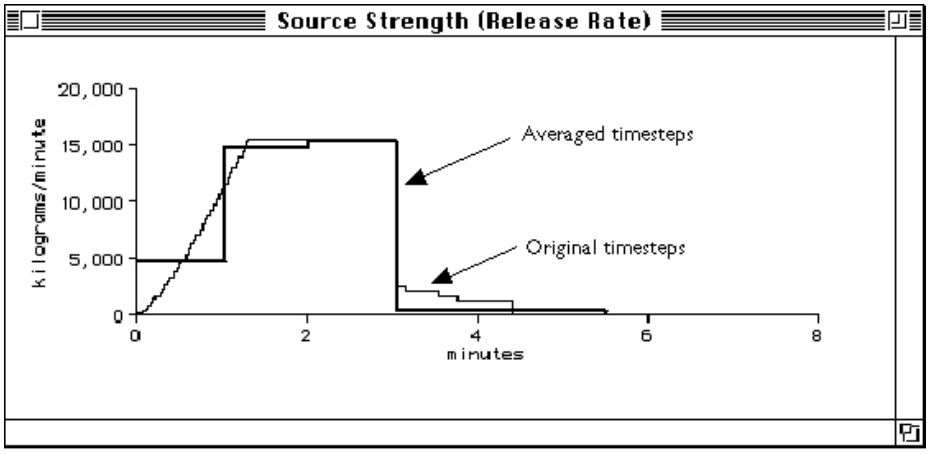

Figure 1. An example of ALOHA's timestep averaging scheme. ALOHA originally estimated source strength for this release in a series of 100 timesteps; these were averaged to four timesteps for use in predicting dispersion.

3.2 DIRECT SOURCE

A direct source option allows the user to directly specify the amount of chemical vapors introduced into the air from a point in space. The user can specify an instantaneous release, or a steady-state release of finite duration. This option can be used with gases that are denser than air and are affected by gravity, or gases that behave as neutrally buoyant. ALOHA allows for a release above ground level for gases that behave as neutrally buoyant.

3.3 PUDDLE SOURCE

Using the Puddle Option, users can model the evaporation of volatile chemicals from a puddle of fixed area. A limited number of mixtures containing a toxic chemical mixed with water or a non-volatile solvent can be modeled. In these cases the evaporation and transport of only the toxic component is modeled. ALOHA uses one of two methods for finding the evaporation rate depending upon whether or not the puddle is sufficiently close to its boiling point. Brighton's formulation (Brighton 1985) is used when the average puddle temperature is sufficiently below its boiling point, and an energy balance method is used when the puddle approaches its boiling point.

The volatilization rate of non-boiling puddles is governed primarily by the wind speed, area of the puddle, and vapor pressure of the chemical,[2] or partial pressure in cases involving mixtures. ALOHA accounts for changes in temperature and composition, in cases involving mixtures. Temperature is held at the boiling point for boiling puddles, and the volatilization rate is defined by the energy balance. Turbulent diffusion is expected to be the primary mechanism transporting vaporized material away from the puddle. Temperature and composition are assumed to be spatially uniform throughout the puddle. As evaporation removes material, the puddle is assumed to grow thinner, but its radius is assumed to be constantALOHA accommodates spills of volatile chemicals on a variety of solid surfaces and on bodies of water. ALOHA assumes that the spilled liquid does not penetrate into the soil, sink, or dissolve in water.

The methods used to compute evaporation rates from puddles of fixed area are also used with the Tank Option to estimate evaporation rates from expanding puddles from liquid leaking from a Tank. The modifications to accommodate spreading puddles are described in section 3.4.

3.3.1 EVAPORATION FROM NON-BOILING PUDDLES

When the average puddle temperature is below its ambient boiling point,[3] ALOHA uses a model by Brighton (Brighton 1985) to predict the evaporation rate. The model assumes that the layer of air

[2] The vapor pressure is strongly dependent upon the puddle **skin temperature**, which can be significantly lower than the temperature of the underlying liquid. Kawamura and Mackay (Kawamura et al. 1985) measured skin temperatures that were 5 to 6°C lower than bulk temperatures in the same puddles. ALOHA approximates the temperature of the puddle as spatially uniform set to the spatially averaged puddle temperature; this can cause ALOHA to overestimate evaporation rates.

[3] ALOHA defines the upper temperature limit for Brighton's model when the correction factor for highly volatile liquids reaches 4.

in contact with the surface of the puddle holds vapors in equilibrium with the liquid in the puddle. As a turbulent airstream passes across the pool surface, vapor molecules diffuse passively from the top of this vapor layer and are advected downwind.

Brighton formulated an expression for the evaporative mass flux, $E(x,t)$, in terms of the friction velocity of the air, U_*, the chemical's vapor-phase saturation concentration, C_s, and a dimensionless mass transfer coefficient, $j(x)$:

$$E(x,t) = C_s U_* \, j(x).$$

The mass transfer coefficient is spatially dependent on the position along the axis oriented parallel to the wind direction. By integrating the mass transfer coefficient over the puddle dimension,[4] a spatially averaged mass transfer coefficient, $\bar{j}$, is found using

$$\bar{j} = \frac{1}{D_P} \int_0^{D_P} j(x)\, dx.$$

As the vapor pressure of the puddle, P_v, approaches ambient air pressure, P_a, the evaporating vapors perturb the boundary layer and affect the turbulent diffusion above the puddle. A correction for highly volatile liquids is applied to the mass transfer coefficient to account for this behavior:

$$\bar{j}_c = -\bar{j} \, \frac{P_a}{P_v} \ln\left(1 - \frac{P_v}{P_a}\right).$$

The total evaporative flux is based on the corrected, spatially-averaged mass transfer coefficient, $\bar{j}_c$:

$$\bar{E}(t) = C_s U_* \, \bar{j}_c.$$

ALOHA estimates the friction velocity, U_*, using a formulation from Deacon (Deacon 1973) for neutral conditions over the ocean described as

$$U_* = 0.03U\left(\frac{10}{z}\right)^n,$$

where U is the user-specified wind speed at height, z.

[4] The diameter of a uniform circular puddle, D_P, is used as the puddle dimension along the along-wind axis.

ALOHA uses a power-law wind speed profile to approximate the wind speed profile above the pool surface. The values of the power-law exponent, n, are shown in Table 7, for the six Pasquill stability classes (Havens and Spicer 1985).

Table 7. Values for the power-law exponent for six Pasquill stability classes.

Stability Class	n
A	0.108
B	0.112
C	0.120
D	0.142
E	0.203
F	0.253

The average mass transfer coefficient is expressed in terms of dimensionless variables as

$$\bar{j} \approx \frac{k}{Sc_T}(1+n)\left[\begin{array}{l}\frac{1}{2}-\frac{1}{\pi}\arctan\left(\frac{\ln\left(e^{\Lambda}X_1\right)}{\pi}\right)+\frac{1-\gamma_e}{\ln^2\left(e^{\Lambda}X_1\right)+\pi^2} \\ +\frac{\left(1+\left(1-\gamma_e\right)^2+\frac{1}{6}\pi^2\right)\ln\left(e^{\Lambda}X_1\right)}{\left(\ln^2\left(e^{\Lambda}X_1\right)+\pi^2\right)^2}\end{array}\right].$$

The dimensionless distance is evaluated at the downwind edge of the puddle as

$$X_1 = \frac{nk^2 D_P}{Sc_T z_0 e^{1/n}},$$

where
k is the VonKarmon constant = 0.4 and
z_0 is the surface roughness length.

Brutsaert (Brutsaert 1982) describes Λ as a measure of the ratio of the scalar roughness length of the puddle and the momentum roughness length of the terrain as

$$\Lambda = \frac{1}{n} + 1 + 2\ln(1+n) - 2\gamma_e + \frac{k}{Sc_T}(1+n)\, f(Sc),$$

where

γ_e is Euler's constant (taken to be 0.577) and

Sc_T is the turbulent Schmidt number set equal to 0.85 in accordance with measurements by Fackrell and Robins (Fackrell and Robins 1982).

The form of $f(Sc)$ depends on the roughness Reynolds number and uses

$$f(Sc) = \begin{cases} \left(3.85 Sc^{1/3} - 1.3\right)^2 + \dfrac{Sc_T}{k}\ln(0.13 Sc) & \text{for} \quad Re_0 < 0.13 : \text{smooth, or} \\ 7.3 Re_0^{1/4}\sqrt{Sc} - 5 Sc_T & \text{for} \quad Re_0 > 2 : \text{rough,} \end{cases}$$

where the roughness Reynolds number, Re_0, is defined by the ratio of the wind friction velocity, U_*, the surface roughness length, z_0, and the kinematic viscosity of air, ν:

$$Re_0 = \frac{U_* z_0}{\nu}.$$

When $0.13 \le Re_0 \le 2$, ALOHA estimates $f(Sc)$ by a straight-line interpolation between the maximum and minimum values of the roughness Reynolds number.

The laminar Schmidt number, Sc, is the ratio of the molecular kinematic viscosity of air to the molecular diffusivity of the contaminant gas in air:

$$Sc = \kappa_c / \nu .$$

Molecular diffusivities of only a few chemicals have been measured. Unless a value has been entered into the chemical library by the user, ALOHA uses Graham's Law to estimate the molecular diffusivity (Thibodeaux 1979)as shown by

$$\kappa_c = \kappa_w \sqrt{M_w / M_c} ,$$

where

M_w is the molecular weight of water,

M_c is the molecular weight of the chemical, and

κ_w is the molecular diffusivity of water vapor in air set equal to 2.39 x 10^{-5} m^2 s^{-1}.

The treatment of evaporation from solutions follows this same method, but the solute and solvent are treated independently using the physical properties of each accordingly. One simplification is used in calculating the dimensionless mass transfer coefficient; the laminar Schmidt number is based on a weighted average molecular weight and a single mass transfer coefficient is used for both solute and solvent.

3.3.2 EVAPORATION FROM BOILING PUDDLES

ALOHA limits the upper bound of the puddle temperature to its ambient boiling point. Non-boiling puddles can absorb enough thermal energy from their surroundings to boil, but it would be extremely rare for a puddle to exceed its boiling point. Users may also set the initial puddle temperature at, but not above, its ambient boiling point. In cases where the calculated puddle temperature approaches boiling, or more precisely, exceeds the upper limit for Brighton's non-boiling puddle model, ALOHA transitions to a boiling puddle model. The model is based on an assumption of a steady-state temperature fixed at the boiling point. The evaporation rate and associated evaporative cooling of the boiling puddle is set equal to a value which balances the thermal energy fluxes, thereby maintaining a constant puddle temperature at its boiling point.

ALOHA allows puddles to transition from boiling to non-boiling, or the reverse. ALOHA constantly compares the evaporation rate calculated with the boiling puddle model with the evaporation rate calculated with Brighton's model at its temperature limit. ALOHA chooses the method that yields the larger evaporation rate.

3.3.3 PUDDLE ENERGY BALANCE

The magnitude of the evaporative mass flux depends on the temperature of the puddle, which is assumed to be spatially uniform. Puddle temperature can increase or decrease with time depending on the magnitude and sign of the six energy sources considered in ALOHA:

- the net shortwave solar flux into the puddle, F_S;
- the longwave radiation flux down from the atmosphere, $F_{\downarrow}$;
- the longwave radiation flux upward into the atmosphere, $F_{\uparrow}$;
- the heat exchanged with the substrate by thermal conduction, F_G;
- the sensible heat flux from the atmosphere, F_H; and
- the heat lost from the puddle by evaporative cooling, F_E.

Energy fluxes into and out of the puddle can either increase or decrease puddle temperature, T_p, as described by

$$\frac{dT_p(t)}{dt} = \frac{1}{\rho_l c_{pl} d_p(t)} \left[F_S + F_{\downarrow} + F_{\uparrow}(t) + F_G(t) + F_H(t) + F_E(t) \right],$$

where

ρ_l is the liquid density,

d_p is the depth of the puddle, and

c_{pl} is the heat capacity of the liquid (J kg^{-1} K^{-1}).

3.3.3.1 Solar Radiation, F_S

The solar irradiance, the flux of solar shortwave radiation at the top of the atmosphere, averages about 1,368 W m^{-2} (Lide 1993). The net transmissivity of the atmosphere is the fraction of solar irradiance that reaches the surface of the earth. Clouds and atmospheric particles both reflect and absorb part of the solar irradiance before it reaches the earth's surface. Frouin et al. (Frouin et al. 1989) reported that the maximum solar flux reaching the surface at continental and maritime locations varied from 1,090 to 1,130 W m^{-2}, indicating that atmospheric transmissivity at these locations ranged from about 80 to 83 percent.

ALOHA estimates the solar radiation flux that reaches the ground at a location, given degree of cloudiness, time, and date (Raphael 1962) as

$$F_s = \begin{cases} 1111\left(1 - 0.0071 C_I^2\right)\left[\left(\sin \varphi_S\right) - 0.1\right] & : \quad \sin(\varphi_S) > 0.1, \\ 0 & \text{otherwise,} \end{cases}$$

where

C_I is the cloudiness index (fraction of sky covered by clouds on a scale of 0 to 10) and

φ_S is the solar altitude (the angle of the sun above the local horizon).

This formula includes a correction for the fraction of solar radiation that is reflected back into the atmosphere based on an average value for the earth's albedo. ALOHA computes solar altitude as a function of latitude, longitude, the time of day, and the Julian day of the year. ALOHA approximates the solar radiation as constant over the time of the release.

3.3.3.2 Longwave Radiation, $F_{\uparrow}$ and $F_{\downarrow}$

Any temperature difference that exists between the puddle and the atmosphere can produce a net loss or gain of energy through radiative energy transfer. Radiative (long wavelength) loss is based on the Stefan-Boltzman radiation law,

$$F_{\uparrow} = -\varepsilon\sigma T_P^4,$$

where
ε is the puddle emissivity (set equal to that of water = 0.97) and
σ is the Stefan-Boltzman constant (= 5.67 x 10^{-8} W $m^{-2}K^{-4}$).

ALOHA uses the following equation developed by Thibodeaux (ref. 1979) to estimate longwave radiation downward from the atmosphere into the puddle:

$$F_{\downarrow} = (1-r)B\sigma T_a^4,$$

where
r is the surface reflectivity to longwave radiation (set to that of water = 0.03),
T_a is the air temperature, and
B is the atmospheric radiation factor, which is a function of partial pressure of water vapor, e_w (Pa), and cloud cover: $B = a + b\,e_w$.

Table 8. Radiation factor coefficients as a function of the cloudiness index C_I.

C_I	a	$b \times 10^6$
0	0.740	44.3
1	0.750	44.3
2	0.760	44.3
3	0.770	44.2
4	0.783	40.7
5	0.793	40.5
6	0.800	39.9
7	0.810	38.4
8	0.820	35.4
9	0.840	31.0
10	0.870	26.6

The partial pressure of water in the atmosphere, e_w (Pa), can be derived from the relative humidity, RH, and air temperature, T_a, as

$$e_w = 99.89 \frac{RH}{100} \exp\left(21.66 - \frac{5431.3}{T_a}\right).$$

3.3.3.3 Heat Exchange with the Substrate, F_G

The substrate, whether ground or water, can be a large source of thermal energy for a puddle. To estimate F_G, ALOHA requires an initial value for ground or water temperature, T_G. This should be a value for the temperature far enough below the surface that temperature is relatively unaffected by daily changes in solar radiation, rather than the surface temperature. When a general range for substrate temperature is known or suspected, choosing a relatively high value from within this range represents a conservative choice because it can result in a higher evaporative flux estimate. In most cases, inaccuracies of a few degrees in either direction in an estimate of T_G are expected to have little effect on predicted evaporation rates.

3.3.3.3.1 SPILLS ON WATER

ALOHA can model insoluble floating liquids spilled on water that is warmer than 5°C. In cases where the puddle temperature is greater than the underlying water, heat flow to the water is neglected. This simplification acts to produce larger evaporation rates, but the effect tends to be short-lived because evaporative cooling often quickly lowers the temperature of the puddle to that of the water.

In cases where the puddle temperature is less than the underlying water, thermal energy flows from the water to the puddle. Convective heat exchange can generate a large sustained heat flux. Modeling the convective process in the water column is beyond the scope of ALOHA, so a simple empirical model is used to estimate the heat transfer based on the temperature difference between the water and the puddle, ΔT. The model was proposed by Webber (Webber 1991), and matches measured results for butane on water:

$$F_G(t) = 500 \frac{W}{m^2 K} \Delta T .$$

3.3.3.3.2 SPILLS ON LAND

The heat exchange between a puddle and a solid substrate is limited by the conductive heat flow within the substrate and is described by Fourier's Law,

$$F_G(t) = -\alpha_G \left. \frac{\partial T}{\partial z} \right|_{z=0} ,$$

where α_G is the thermal conductivity of the ground.

The temperature gradient is a function of time and is found by solving time dependent heat equation for the ground temperature,

$$\frac{1}{\kappa_G}\frac{\partial T}{\partial t} = \frac{\partial^2 T}{\partial z^2},$$

where κ_G is the thermal diffusivity of the ground. The ground is represented by a slab of finite thickness, infinite in the horizontal directions. The thickness of the slab is based on an estimate of the depth over which the temperature is affected by the puddle. We assume that the ground is initially at a uniform temperature, the interface with the puddle is at the temperature of the puddle, and the other interface is at the initial ground temperature. The heat equation has a simple analytical error-function solution when the puddle temperature is constant; however, when the puddle temperature varies with time, the solution becomes more complicated, so the heat equation and heat flux expressions are solved numerically using a forward-stepping finite difference method.

The distance between nodes is adjusted to assure numerical stability, minimize numerical error, and manage the computational time. To insure numerical stability the following condition should be met:

$$dz \geq \sqrt{3\kappa_G dt}\,.$$

The depth over which the ground temperature is affected by the puddle is approximated by finding the depth at which the ground temperature changes by one degree after one hour, assuming a constant puddle temperature. If the initial temperature differential between the puddle and ground is small, a minimum of 20°C is used to estimate the affected depth.

Comparison between this heat transfer model and experimental data suggests that a correction factor is needed for the effective thermal conductivity of soils (Briscoe and Shaw 1980). The effective thermal conductivity appears to be about 9 times that of the measured values for soils.

Table 9. Thermal properties of solid substrates with correction factor applied (Briscoe and Shaw 1980).

	Thermal Conductivity ($Wm^{-1}K^{-1}$)	***Thermal Diffusivity ($m^2 s^{-1}$)***
Dry Sandy Soil	2.34	1.74×10^{-6}
Concrete	8.28	3.74×10^{-6}
Default Soil	8.64	4.13×10^{-6}
Moist Sandy Soil	5.31	3.02×10^{-6}

3.3.3.4 Evaporative Heat Flux

The evaporative heat flux, F_E (J m^{-2}), represents the effect of evaporative puddle cooling. Once the average evaporative flux, $\overline{E}$ has been estimated, ALOHA estimates F_E as $F_E = L_C \overline{E}$, where L_C (J kg^{-1}) is the specific latent heat of vaporization for the chemical at the puddle temperature.

3.3.3.5 Sensible Heat Flux

The sensible heat flux, F_H, is the thermal conduction to or from the air as a result of temperature differences between the puddle and the air above it (Brighton 1985, 1990), and is shown as

$$F_H = \rho_a c_{p,a} C_H U_* \left(T_a - T_p \right),$$

where

ρ_a is the density of air (kg m^{-3}),

$c_{p,a}$ is the heat capacity of air (J kg^{-1} K^{-1}), approximated as a constant 1,004 J kg^{-1} K^{-1}, and

C_H is the sensible heat transfer coefficient = $\overline{j}_c \left({thermal\ diffusivity} \big/ {molecular\ diffusivity} \right)^{2/3}$.

3.4 CHEMICALS RELEASED FROM A TANK

ALOHA can estimate the amount of substance released into the air as a result of a rupture of a tank. ALOHA treats tanks containing pressurized gases, liquids at ambient pressure, gases liquefied by refrigeration, and gases liquefied under pressure. ALOHA deals only with tanks containing a single chemical. It does not deal with tanks that are pressurized with a second substance such as air or an inert gas. As material is released from the tank, ALOHA reevaluates the conditions within the tanks and can change the release rate calculation as needed.

The rate at which a chemical enters the atmosphere is limited, but not entirely determined, by the rate at which the chemical is released from the tank. The release rate from the tank depends upon the phase released (liquid, gas, or mixed phase), the driving pressure, and the nature of the rupture.

Two types of ruptures can be modeled: a hole in the tank wall, or a release through a short pipe or valve. Models for a release through a hole are used for both types of ruptures when a gas or non-boiling liquid are involved; they provide reasonable overestimates for short pipes. However, for superheated liquids and 2-phase fluids, the release rate through a hole and short pipe can differ significantly, so the release rate model differentiates these two rupture types.

In tanks containing liquids, the release point can occur above the level of the liquid, below the level of the liquid, or at the level of the liquid. The location of the rupture largely determines the pressure driving the release and the phase of the effluent. Top vents are assumed to be absent.

Material released from a hole or short pipe can be a gas, a non-boiling liquid, a superheated liquid, or a mixture of liquid and gas. ALOHA predicts that a released gas enters the atmosphere immediately and disperses downwind, or ignites to form a jet fire. ALOHA predicts that a liquid released at a temperature below its boiling point forms a puddle which then evaporates to generate an airborne cloud. So, for non-boiling liquids, the tank release rate is linked to a puddle evaporation model. ALOHA does not allow the user to model a pool fire that starts with a tank release. ALOHA assumes that a superheated liquid (liquids released at a temperature above their ambient boiling point) enters the atmosphere immediately and disperses downwind, or ignites to form a jet fire. We expect that in many cases a superheated liquid would partially rain out to form a puddle; however, ALOHA employs this assumption to ensure that it can provide a reasonable overestimate of the actual source strength.

3.4.1 INTERNAL TEMPERATURE OF THE TANK

The temperature at the onset of the release is defined by the user.

To account for temperature changes during the release, ALOHA considers thermal conduction through the tank walls that are in contact with liquid contents, and evaporative cooling due to liquid vaporizing within that tank to fill the void created by the escaping fluid. (Cooling due to adiabatic expansion of a gas within a tank is neglected.) This is shown as

$$\frac{\mathrm{d}T_T}{\mathrm{d}t} = \frac{Q_e L_c + F_{Hw} A_{tw}}{\rho_l c_{pl} V_l},$$

where

F_{Hw} is the thermal energy flux across the walls,

A_{tw} is the area of the tank walls in contact with liquid, and

ρ_l, c_{pl}, V_l are the density, heat capacity, and volume of the liquid within the tank.

The mass evaporation rate into the head space of the tank, Q_e, is simply related to the total mass loss from the tank, Q_T, and the density of the effluent fluid, ρ_X, and is determined using

$$Q_e(t) = \frac{Q_T}{\rho_X}\left(\frac{\rho_l \rho_g}{\rho_l - \rho_g}\right),$$

where ρ_g is the density of the gas.

The thermal energy flux across the walls of the tank that are in contact with the liquid contents assumes that the tank walls are constructed of 2 cm of steel and 10 cm of insulating foam.

3.4.2 INTERNAL PRESSURE OF THE TANK

Tanks are assumed to be unvented and initially contain a single component that is in thermodynamic equilibrium with its own vapors in the headspace (ALOHA does not allow for tanks containing other gases in the head space). For tanks containing liquid, the internal pressure is defined by the tank temperature and set equal to the vapor pressure of the liquid. Tanks containing only gas have an additional degree of freedom, so the user must define the initial temperature and pressure of the tank.

3.4.3 PHASE OF THE EFFLUENT FROM THE TANK

For tanks containing pressurized gases, or liquids stored below their boiling points, the phase of the effluent is easily determined from the location of the rupture. However, for tanks containing superheated liquids, the determination of the phase of the effluent can be complicated when the rupture occurs in the head space. When a rupture is in or intersects the headspace of a tank containing a liquid stored above its normal boiling point, pressure is quickly released causing the liquid to vaporize quickly. This process can result in the formation of bubbles throughout the liquid (homogeneous nucleation). If gas bubbles are generated faster than they can rise and pass out of the liquid, the volume of the fluid can swell and fill the tank. The rupture in the head space can then release a 2-phase mixture of gas and liquid resulting in a large release. In most cases, ALOHA assumes that any rupture in the head space of a tank containing a liquid stored above its boiling point will swell to fill the tank with a uniform bubbly 2-phase mixture. However, there are two chemicals in ALOHA for which a more refined model is used to predict swelling: ammonia and chlorine.

Ammonia and chlorine are treated differently than other gases liquefied under pressure. Instead of assuming that a rupture in the head space always results the vessel filling with a uniform 2-phase mixture, ALOHA uses a vapor disengagement calculation. The DIERS method (Fisher et al. 1992) compares the superficial vapor velocity to the drift flux to determine whether the fluid swells to fill the vessel. The superficial vapor velocity is defined as the volume release rate divided by the cross sectional area of the vessel and can be interpreted as the speed at which a slug of vapor must travel upward through the cylinder to match the release rate of the exit port. The drift flux of the boiling 2-phase fluid can be interpreted as the volume flux of gas bubbles in the boiling fluid relative to the average flow velocity of the fluid (in ALOHA the fluid is approximated as stationary). At the surface of the 2-phase fluid, the drift flux can be viewed as the gas flux through the surface.

The drift flux is the product of two terms, the bubble rise velocity, U_{rise}, and the reference dimensionless superficial vapor velocity, Ψ. These two terms are found from empirical studies and take different forms depending on the flow regime. According to Leung (Leung 1994) most single component liquids exhibit churn-turbulent (CT) flow. The measurements of the flow behavior of ammonia made by Fauske and Associates and transmitted to us by Karlins (Karlins 1994) suggests that ammonia behaves as a CT fluid. Our assumption that chlorine behaves as a CT fluid is based solely on Leung's expectation and is not based on empirical data. For CT flow, the bubble rise velocity is defined as

$$U_{rise} = 1.53 \frac{\left[\sigma g \left(\rho_l - \rho_g\right)\right]^{1/4}}{\rho_l^{1/2}},$$

where
σ is the surface tension,
ρ_l is the density of the liquid phase,
ρ_g is the density of the gas phase, and
g is the acceleration of gravity.

The reference dimensionless superficial vapor velocity depends on the average void fraction of the 2-phase fluid and is defined as

$$\Psi = \frac{2\alpha}{1 - C_0 \alpha},$$

where
α is the average void fraction and
C_0 is the correlating parameter (= 1.0 for conservative estimate).

If the superficial vapor velocity is greater than the drift flux ($U\Psi$), then the 2-phase fluid is predicted to swell. Since the drift flux depends on the average void fraction, it varies as the fluid swells and changes volume. If, at the point where the fluid fills the vessel, the drift flux is still less than the superficial vapor velocity, then 2-phase venting is predicted. As material is lost, the average void fraction of the fluid changes, and when the superficial vapor velocity becomes less than the drift flux, 2-phase venting is predicted to cease. Generally, small leaks lead to gas release and larger leaks lead to 2-phase venting.

The DIERS approach described above was developed for vertically oriented cylinders of constant cross section with a release point at the top of the cylinder. Grolmes and Fisher (Grolmes and Fisher 1994) recommend, as an acceptable approximation, modeling spherical and horizontal-cylindrical vessels as vertical cylinders of equivalent volume and height. ALOHA accommodates vessels with ruptures below the top of the vessel by modeling these systems as vertical cylinders with heights equal to the height of the actual exit port and a volume equal to the volume of the actual vessel below the level of the exit port.

3.4.4 RELEASE OF A LIQUID STORED BELOW ITS AMBIENT BOILING POINT

The following method is applied to holes and short pipes below or intersecting the level of the liquid in a tank containing a liquid stored below its ambient boiling point. ALOHA calculates the release of the liquid from the tank, the puddle formation, and the evaporation rate from the puddle. When the liquid level drops below the bottom of the hole or pipe, ALOHA neglects any further release of gas from head space above the liquid. The same calculation methods are used for a hole in the tank wall and a short pipe.

3.4.4.1 Mass flow rate

ALOHA uses Bernoulli's equation to compute the mass flow of liquid from the hole,

$$Q_T(t) = C_{dis} A_f \left(2\left(P_h - P_a\right)\rho_l\right)^{1/2},$$

where C_{dis} is the discharge coefficient (0.61),

A_f is the area of the hole times the fraction of the hole lying below the level of the liquid,

P_a is the ambient atmospheric pressure, and

P_h is the internal pressure in the tank at the height of the hole.

ALOHA assumes that the tank is not vented. When the liquid level is above the top of the hole, the internal pressure driving the flow, P_h, is the combination of the vapor pressure of the liquid and the hydrostatic pressure of the liquid above the hole. However, as the liquid level drops, the internal pressure calculated in this manner can approach the ambient air pressure causing the flow to stop. Commonly, air can be ingested back into the tank allowing flow to continue as a series of gushes. To approximate this in ALOHA, when the computed value for P_h reaches 1.01 P_a, it is held constant at that value (Belore and Buist 1986, Dodge, Bowels, and White 1980).

When the liquid level intersects the hole, the internal pressure at the hole is the ambient air pressure plus the hydrostatic pressure of the liquid above the bottom of the hole.

3.4.4.2 Puddle Growth

The liquid release creates a spreading puddle that evaporates or burns. Evaporation or burning acts to reduce the mass of a puddle that has been formed. The mass loss is approximately proportional to the area of the puddle. When the tank release rate is greater than the computed evaporation rate, ALOHA predicts that the puddle will spread. As the puddle evaporates, ALOHA does not permit the puddle's area to shrink; it allows the puddle depth to decrease. For spreading puddles, ALOHA uses the method proposed by Briscoe and Shaw (Briscoe and Shaw 1980) to compute the radius of the puddle, r_p, which is described as

$$\frac{dr_p}{dt} = \sqrt{2gd_p},$$

where d_p is the depth of the puddle.

ALOHA approximates the puddle depth as uniform and terminates the spreading when the depth drops to 5 mm, an arbitrarily chosen value.

3.4.4.3 Puddle Temperature

The temperature of the puddle has a large impact on the evaporation rate. In addition to the sources and sinks of thermal energy described in the section on the Puddle Option, liquid added to the puddle from the tank can either raise or lower the average temperature of the puddle. The change in the puddle temperature is defined by the sum of the thermal flux terms:

$$\frac{\mathrm{d}T_p(t)}{\mathrm{d}t} = \frac{1}{\rho_l c_{pl} d_p(t)}\left[F_S + F_{\downarrow}(t) + F_{\uparrow}(t) + F_G(t) + F_H(t) + F_E(t) + F_{dM}(t)\right].$$

The thermal energy flux from the addition of liquid from the tank, F_{dM}, is proportional to the temperature difference between the liquid in the tank and that in the puddle, and is described as

$$F_{dM}(t) = \frac{Q_T c_{pl}(T_T - T_P)}{\pi r_p^2},$$

where Q_T is mass flow rate into the puddle.

The thermal energy flux from the ground for a growing puddle is modeled in a way that is conceptually consistent with the stand-alone puddle. The puddle is modeled as discrete concentric rings of liquid in contact with the ground; as the puddle expands rings are added. The entire puddle is assumed to be a uniform temperature, but the underlying ground temperature varies depending upon its duration of contact with the puddle. Conduction through the ground is treated separately for each ring; the thermal energy flux is the sum of the individual heat flux terms from each ring.

As with the puddle scenario described above, ALOHA uses one of two methods for finding the evaporation rate depending upon whether the puddle is sufficiently close to its boiling point.

Brighton's formulation is used when the average puddle temperature is below its boiling point, and an energy balance method is used when the puddle approaches its boiling point.

3.4.5 RELEASE OF A 2-PHASE MIXTURE OR A LIQUID ABOVE ITS AMBIENT BOILING POINT

ALOHA uses the Homogeneous Nonequilibrium Model for release scenarios involving an effluent that is a superheated liquid, or a 2-phase mixture resulting from the flash boiling of a superheated liquid (Fauske 1985, Fauske and Epstein 1987, Henry and Fauske 1971). The mass flux, G, through a short pipe or hole is described by

$$G = \frac{L_c}{\left(v_g - v_l\right)}\left(Nc_P T\right)^{-1/2},$$

where,

L_c is the specific latent heat of vaporization (J/kg),

v_g is the specific volume of the vapor (m^3/kg),

v_l is the specific volume of the liquid (m^3/kg),

c_p is the heat capacity of the fluid (J/kgK),

T is the temperature (K),

$$N = \frac{L_c^2 v_l}{2\Delta P C_{dis}^2 \left(v_g - v_l\right)^2 T c_P} + \frac{l}{l_e},$$

ΔP is the difference between inside and outside pressure (Pa),

l is the length of the pipe (m), and

l_e = 0.1 m.

The Homogeneous Nonequilibrium Model is limited to a 2-phase flow that is predominately liquid. The maximum value of Quality, X, for which the Homogeneous Nonequilibrium Model is valid (Quality is defined as the mass of the vapor divided by the mass of the mixture.) is

$$X(\max) = \frac{P c_P T \left(v_g - v_l\right)}{L_c},$$

where P is the pressure of the fluid within the tank.

When the Quality of the effluent exceeds this limit, ALOHA computes the release rate based on a fixed quality set to $X(\max)$. This provides a reasonable overestimate of the actual release.

The Homogeneous Nonequilibrium Model was developed to treat release scenarios involving pipes that are shorter than 10 cm, including a pipe length set to zero and a hole in the tank wall. ALOHA allows the user to specify whether the release is through a hole or short pipe, the latter corresponds

to a pipe length of 10 cm, the upper limit of the model. At the lower limit of pipe length, the Homogeneous Nonequilibrium Model reduces to the Bernoulli equation. At the upper limit of pipe length, 10cm, the Homogeneous Nonequilibrium Model approximately reduces to the homogeneous equilibrium model, which has been shown to be applicable to typical valve geometries (Huff 1985).

For holes in a tank wall, the Homogeneous Nonequilibrium Model predicts that the release rate is proportional to the density and pressure difference at the exit port. In contrast for 10 cm pipes, the Homogeneous Nonequilibrium Model is insensitive to both density and pressure differential. Flashing is assumed to occur in the pipe resulting in choked flow. As a result, release rates of superheated liquids through short pipes are generally much smaller than through holes.

Upon release from the tank, ALOHA assumes that the liquid undergoes an adiabatic vaporization. Evaporation cools the liquid as it vaporizes. If the liquid has not vaporized completely before its temperature drops to its ambient boiling point, ALOHA assumes that the cold 2-phase mixture is in the form of a fine aerosol and treats it as a dense gas. ALOHA does not allow the liquid to rain out and form a puddle.

The Homogeneous Nonequilibrium Model is limited by the diameter of the pipe. For large diameter pipes, ALOHA uses an approximation to insure that the predicted release rate does not underestimate the actual rate. For pipes greater than one meter in diameter, ALOHA reverts to the Bernoulli equation. For pipe diameters between 0.1 and 1 meter, ALOHA interpolates between the Homogeneous Nonequilibrium Model and the Bernoulli equation.

3.4.6 GAS RELEASE THROUGH A HOLE OR SHORT PIPE

ALOHA predicts a gas release under two conditions: the tank contains a pressurized gas, or there is a small leak in the head space containing chlorine or ammonia liquefied under pressure. ALOHA uses a single model which produces identical source strength estimates for holes and pipes regardless of which rupture type its user chooses. ALOHA considers the release rate from ruptures in the head space of tanks containing liquids stored below their boiling points as insignificant.

ALOHA uses algorithms incorporated in LEAKR, a computer model developed for Environment Canada (Belore and Buist 1986), to predict the release rate of gases from holes and short pipes. From the ratio of tank to atmospheric pressure, the ratio of hole width to tank length, and the critical pressure ratio for sonic flow (a threshold pressure ratio value), ALOHA first determines whether gas flow will be supersonic (choked) or subsonic (unchoked). If the pressure difference is great enough, ALOHA models flow as supersonic until the pressure drops to the point at which flow is subsonic. From then on, ALOHA computes a subsonic release rate until it predicts that tank pressure has dropped to atmospheric pressure. The estimated rate of gas release drops over time because the tank pressure is expected to drop as gas exits the tank, and because adiabatic expansion is expected to cool the tank contents, further reducing pressure. In gas release cases, ALOHA does not account for the effect of heat flux across the tank wall or for frictional differences between tank holes and short pipes/valves.

ALOHA predicts whether gas outflow will be either subsonic or supersonic by computing three ratios. The first is the ratio of atmospheric pressure to tank pressure:

$$R_P = P_a / P_T .$$

The second important ratio is the ratio of hole diameter to tank diameter,

$$\beta_c = l_h / l_T ,$$

where

l_T is the diameter of a spherical or cylindrical tank, and

l_h is the either the diameter of a round hole or the square root of the area of a rectangular hole.

The third important ratio is the critical pressure ratio,

$$R_c = \left(\frac{2}{\gamma + 1} \right)^{\frac{\gamma}{\gamma - 1}} \qquad \beta_c > 0.2 \qquad \text{(big hole)}, \text{ and}$$

$$R_c^{\frac{1-\gamma}{\gamma}} + \frac{\gamma - 1}{2} \beta_c^4 R_c^{\frac{2}{\gamma}} = \frac{\gamma + 1}{2} \qquad \beta_c \le 0.2 \ \text{(small hole)},$$

where γ is the ratio of gas heat capacity at constant pressure and gas heat capacity at constant volume.

3.4.6.1 Choked Flow

When R_P is less than or equal to R_c, mass flows from the tank at the speed of sound and is usually choked, so that reducing downstream pressure further does not appreciably change the flow rate. The mass flow rate is given by

$$Q(t) = C_{dis} A_h \sqrt{\rho_g(t) P_T(t) \gamma \left(\frac{2}{\gamma + 1} \right)^{\frac{\gamma + 1}{\gamma - 1}}} .$$

3.4.6.2 Unchoked Flow

When R_P is greater than R_c, the flow is subsonic and the mass flow is given by

$$Q(t) = C_{dis} A_h \sqrt{2\rho_g P_T \frac{\gamma}{\gamma - 1}\left(\left(\frac{P_a}{P_T}\right)^{2/\gamma} - \left(\frac{P_a}{P_T}\right)^{(\gamma+1)/\gamma}\right)}.$$

Outside the tank, the gas expands until its pressure equilibrates with the atmosphere. This process is modeled as an adiabatic expansion with an associated reduction in temperature. The temperature of the gas after the gas has fully expanded is given by

$$T_g = T_T \left(\frac{P_T}{P_a}\right)^{\frac{1-\gamma}{\gamma}}.$$

Detailed discussions on the relationship between choked and unchoked flow is given by Shapiro (Shapiro 1953) and Blevins (Blevins 1984). How this relationship can be applied to hazard analysis is discussed by Hanna and Strimaitis (American Institute of Chemical Engineers. Center for Chemical Process Safety. 1989).

3.5 GAS PIPELINE

3.5.1 GENERAL COMMENTS

Only pure gas releases from pipe ruptures are considered by ALOHA. ALOHA's gas pipeline algorithm is based on modifications made by Wilson (Wilson, Alberta. Pollution Control Division., and University of Alberta. Dept. of Mechanical Engineering. 1981, Wilson et al. 1979) to a model developed by Bell (Bell 1978). Measurements show that heat transfer to the moving gas through the pipe walls maintains an almost isothermal condition throughout the length of the pipe except for the last 200 hole diameters. Within 200 diameters of the hole, the flow is assumed to be adiabatic because of the large acceleration near the end of the pipe.

3.5.2 THEORY

Wilson showed that an exponential is a solution for isothermal quasi-steady state pipe flow, and that the release of gases from a finite length of pipe can be approximated by a double exponential of the form

$$Q(t) = \frac{Q_0}{(1+\alpha)}\left(e^{-t/\alpha^2\beta} + \alpha e^{-t/\beta}\right),$$

where

Q is the rate of mass discharge per unit time (kg s^{-1}),

Q_0 is the initial mass flow at the time of the rupture (kg s^{-1}),

α is a non-dimensional mass conservation factor, and

β is the release rate time constant (s).

The pressure in most pipelines is much greater than ambient pressure. Therefore, Q_0 is calculated assuming a choked flow condition, where, for a pipe, the discharge coefficient is one and the internal pressure and temperature at the time of rupture are known, using

$$Q_0 = P_0 A_h \sqrt{\frac{\gamma MW}{RT_g}\Gamma^{-1}},$$

where

P_0 is the initial pipe pressure (Pa),

A_h is the area of the hole (m^2),

MW is the molecular weight of the gas (kg/mole),

γ is the ratio of the heat capacity at constant pressure to heat capacity at constant volume, and

$$\Gamma = \left(\frac{\gamma+1}{2}\right)^{\frac{\gamma+1}{\gamma-1}}.$$

The time constant, β, is computed by the equation (Wilson 1989),

$$\beta = \frac{2}{3}\tau_p K_F \Gamma^{3/2} K_H^{-3}\left[\left(1+\frac{K_H^2}{K_F\Gamma}\right)^{3/2}-1\right],$$

$$\tau_p = L_p \big/ c\,,$$
$$K_F = d_p \big/ \left(\gamma\mu L_p\right), \text{ and}$$
$$K_H = A_h \big/ A_p\,,$$

where
L_p is the length of the pipe,
c is the speed of sound in the pipe,
d_p is the pipe diameter,
μ is the Darcy-Weisbach friction factor, and
A_p is the cross-section area of the pipe.

The speed of sound for an isothermal pipe is

$$c = \left(\frac{\gamma RT}{MW}\right)^{1/2}.$$

The friction factor is computed according to Blevins (Blevins 1984) as

$$\mu = \frac{0.25}{\left(0.57-\log\left(\varepsilon/d_p\right)\right)^2},$$

where the roughness coefficient, ε, is set to 0.0001 m for normal conditions and is increased to 0.002 m for rough pipe conditions. For typical pipe conditions, $0.01 < \mu < 0.02$.

The time constant can be simplified for small- and large-hole conditions. When $\left(K_H^2 \big/ K_F\Gamma\right)$ is small, the pipe can be treated like a long isothermal storage tank:

$$\beta \approx \tau_p K_H^{-1}\sqrt{\Gamma} \quad \text{(small hole)}.$$

A hole is considered to be large if $\left(K_H^2 \big/ K_F\Gamma\right) > 30$ and

$$\beta \approx \frac{2}{3}\tau_p\sqrt{K_F} \quad \text{(large hole)}.$$

The total mass in the pipeline is based on the ideal gas law,

$$M_T = \frac{P_0 A_p L_p MW}{RT},$$

and the mass conservation factor is

$$\alpha = \frac{M_T}{\beta Q_0}.$$

For each time step, the exit temperature must be re-evaluated by the methods described below. Adiabatic decompression of the gas within 200 diameters of the hole is assumed. Beyond 200 diameters of the hole, the flow is approximately isothermal with frictional heating and adiabatic cooling in near balance. The exit temperature of the current time step is given by

$$T_f = T_g \left(\frac{P_a}{P_{ia}} \right)^{(\gamma-1)/\gamma},$$

where

T_g is the exit temperature at the previous step,

P_a is the ambient air pressure, and

P_{ia} is the pressure at the isothermal-adiabatic interface, $P_{ia} = Qc / A_p$.

At the isothermal-adiabatic interface, for steady-state conditions, the model assumes an infinite reservoir attached to a finite length of pipe with the hole the same size as the pipe. For this case, the flow rate is calculated as

$$Q = A_p \rho_{ia} v_{ia},$$

where v_{ia} is the velocity of the gas at the isothermal-adiabatic interface, and ρ_{ia} is the density at the interface. Choked flow is assumed and leads to the relationships

$$v_{ia} = c/\gamma \text{ and}$$

$$\rho_{ia} = \rho_r P_{ia} / P_r,$$

where the subscript *r* refers to the reservoir. A non-linear equation for the velocity of the gas out of the reservoir must be solved to find a value for P_{ia} to be used in the above equation. If Ma is the Mach number (ratio of discharge speed to the speed of sound), the equation for isothermal pipe flow is (Blevins 1984)

$$\int_0^{L_p} \frac{\mu}{d_p} \mathrm{d}L = \int_{Ma^2}^{1/\gamma} \left(\frac{1-\gamma Ma^2}{\gamma Ma^4} \right) \mathrm{d}Ma^2 ,$$

where the approximation has been made that the length of the pipe where isothermal flow predominates is much larger than the part where adiabatic flow occurs, so that the upper limit of the left-hand integral is set to be the whole length of the pipe. Integration of this expression leads to an expression for the pipe friction parameter,

$$K_F = \left[\frac{c^2 - \gamma v_{ir}^2}{\gamma v_{ir}^2} - \frac{c^2 - \gamma v_{ia}^2}{\gamma v_{ia}^2} + 21\mathrm{n}\left(\frac{\mathrm{v}_{ir}}{v_{ia}} \right) \right]^{-1} ,$$

where v_{ir} is the gas velocity at the reservoir-pipe interface.

The pipe pressure at the adiabatic-isothermal interface, P_{ia}, is estimated from the relationship

$$P_{ia} = \left(\frac{v_{ir}}{v_{ia}} \right) \left(P_r - \frac{1}{2} \rho_r v_{ir}^2 \right) .$$

3.5.3 COMPUTATIONAL NOTES

The gas pipeline release algorithm computes an array of gas release rates at different times. As in other source routines, the length of the time interval varies such that equal amounts of mass are released in each time step. If n is the total number of time steps, then each new time step is found from the previous one by using a Newton-Raphson iteration scheme to find the roots of the equation,

$$F\left(t_{i+1}\right) = \frac{M_T}{n} - \int_{t_i}^{t_{i+1}} Q(t) \mathrm{d}t ,$$

where t_i is the previous time and t_{i+1} is the new time. Minimum time interval is 60 seconds and the release is terminated if it extends beyond one hour.

4 AIR DISPERSION MODELS

4.1 INTRODUCTION

The accidental release of a volatile chemical can present a threat to life and health far from the point of release. Some chemicals are toxic by inhalation, others can pose a fire hazard. Air dispersion models are central to predicting hazard zones associated with toxic or flammable gas clouds. These models are used to predict how the concentration of a pollutant, once released into the air, varies with time and position. ALOHA provides information about the concentration and duration of exposure, but does not resolve the probability that an exposed individual will be injured.

Vapor clouds containing a flammable chemical mixed with air can burn when an ignition source is present. When a large quantity of a flammable chemical is released into the air and disperses to the point where a flammable fuel/air mixture forms before ignition, the fire can travel from the ignition source to the edges of the flammable cloud. The rate at which the combustion propagates through the cloud determines whether a damaging shock wave is generated (a vapor cloud explosion). The hazards associated vapor cloud explosions are described in Chapter 5. Hazards associated with flash fires, which do not generate damaging shock waves, are described in Chapter 6. The dispersion models described in this chapter are used to estimate the flammable area of the cloud. The movement of the ambient air is responsible for the advection and diffusion of a neutrally-buoyant pollutant in all but the very near field. The movement of pollutants with densities significantly different than the ambient air is also affected by gravity and can loft or hug the ground. But even for dense gases and dense aerosols, the movement of the ambient air usually dominates their dispersion.

A chemical vapor cloud is composed of a pollutant chemical and air in a ratio that changes with time and location. Clouds containing chemicals with high molecular weight, or aerosols, can be sufficiently dense that gravity has a significant effect on their movements. These dense gas clouds are modeled differently in ALOHA than clouds that are not directly affected by gravity. ALOHA incorporates two semi-empirical air dispersion models: the Gaussian model is appropriate for pollutants clouds that are not directly affected by gravity; the Heavy Gas model is appropriate for pollutant clouds with densities greater than the ambient air and affected in a significant way by gravity. These air dispersion models used for neutral and dense pollutant plumes in ALOHA can account for vertical gradients in wind speed and atmospheric turbulence, but do not account for topographic steering or winds that vary with time.

The ambient wind usually dominates the advection and diffusion processes for both dense and neutrally buoyant gas clouds. The movement of air is characterized by its velocity field and turbulence. The roughness elements of the ground provide a drag on the moving air, producing a velocity gradient where the speed at the surface itself is zero and increases logarithmically with height. The surface roughness elements not only affect the vertical wind profile, but also generate turbulence within the wind field. Topography and large structures also affect the velocity field and turbulence as the wind moves around and over these features. Turbulence is also generated by thermal effects; the sun warms the ground which, in turn, warms surface air causing it to rise.

4.2 METHODS FOR CHARACTERIZING WIND FIELDS AND TURBULENCE

Atmospheric turbulence has a major impact on the rate of dispersion of a pollutant cloud. Stability is a concept used to characterize the property of the low-lying atmosphere that governs the vertical movement of air. Specifically, stability refers to the tendency of the atmosphere to resist or enhance vertical motion and thus turbulence. A stable atmosphere inhibits the vertical mixing; a neutral atmosphere neither enhances nor inhibits vertical mixing; and an unstable atmosphere enhances vertical mixing and turbulence. Solar radiation plays a large role in atmospheric stability. With strong solar radiation, the ground warms and warms the low-lying air; the warm air rises generating eddies and a high level of turbulence. In contrast, when the air temperature increases with height, buoyancy forces act to inhibit vertical mixing creating a highly stable atmosphere. Stability classification is a central factor in ALOHA's air dispersion models.

Pasquill (Pasquill 1961) defined six **atmospheric stability classes** (now usually called the Pasquill-Gifford-Turner stability classes). Classes A to F each represent a different degree of atmospheric turbulence. Stability class D represents a neutral stability condition. Unstable conditions are associated with atmospheric stability classes A, B, and C, where A is extremely unstable, B is moderately unstable, and C is slightly unstable. Stability classes E and F represent increasingly stable atmospheric conditions.

ALOHA can use either of two estimation methods to determine atmospheric stability class, depending on whether the user enters weather information manually or a portable weather station transmits readings to it. In addition, ALOHA allows the user to override these methods and directly specify the stability class.

4.2.1 MANUAL DATA ENTRY OF ATMOSPHERIC CONDITIONS

When the user manually enters atmospheric data, ALOHA uses a stability class method that incorporates the Pasquill-Gifford-Turner stability typing scheme. The method was developed using air dispersion measurements collected during experimental releases conducted during the 1950s and 1960s. During these experiments, most concentration measurements were made at distances within 1 kilometer from the release point. Because only in a few instances were concentrations measured at distances as far as 10 kilometers from the release location, it is not certain whether the method is reliable at greater distances.

Solar insolation (the solar energy flux) and wind speed are the two factors affecting the choice of stability class in ALOHA. Table 10 forms the basis for the determination of stability class for plumes over land in ALOHA. This table is identical to one presented by Turner (Turner 1994) with the exception that Turner did not assign stability classes for nighttime cases when wind speed is less than 2 m s^{-1}. According to Turner, strong insolation corresponds to a solar altitude greater than 60° on a clear day, moderate insolation corresponds to a solar altitude between 60° and 35° on a clear day, and slight insolation corresponds to a solar altitude between 15° and 35° on a clear day. Nighttime is considered the time between one hour before sunset to one hour after sunrise.

ALOHA includes solar altitude and cloud cover in its determination of stability class. User-entered information on date, time, location, and cloud cover are used to determine the solar insolation. If

more than one stability class fits the indicated conditions, ALOHA selects the most stable of these classes. ALOHA provides the user the option to directly select the stability class.

Table 10. Solar Insolation and stability class table.

Wind Speed	***Day***			***Night***	
at 10 meters	Solar Insolation			Cloud Cover	
($m\ s^{-1}$)	Strong	Moderate	Slight	>50%	<50%
<2	A	A – B	B	E	F
2 – 3	A – B	B	C	E	F
3 – 5	B	B – C	C	D	E
5 – 6	C	C – D	D	D	D
>6	C	D	D	D	D

Stability is D for completely overcast conditions during day or night.

For plumes over water, ALOHA assumes stable conditions regardless of solar insolation or wind speed.

ALOHA classifies the solar insolation based on the net energy flux to the ground. Solar insolation greater than 851 W/m^2 is considered strong insolation; computed insolation between 851 and 526 W/m^2 is considered moderate insolation; and computed insolation between 526 and 176 W/m^2 is considered slight insolation. ALOHA estimates solar insolation absorbed by the ground from the location, time, and degree of cloudiness (Raphael 1962):

$$F_s = \begin{cases} 1111\left(1-0.0071C_I^2\right)\left(\sin\phi_S - 0.1\right) & \sin(\phi_S) > 0.1 \\ 0 & \text{otherwise} \end{cases}.$$

C_I is the cloudiness index (on a scale of 0 to 10) and

ϕ_S is the solar altitude (the angle of the sun above the local horizon) in degrees.

ALOHA computes solar altitude, ϕ_S, as a function of
the latitude in radians, θ,
the longitude in radians, λ,
the hour of the day in Greenwich Mean Time (GMT) , Z (as 1 to 24 hours),
the Julian day (the day number in the year) in days , J (as 1 to 365 days),

$$\sin(\phi_S) = \sin(\theta)\sin(\delta_S) + \cos(\theta)\cos(\delta_S)\cos(h_s),$$

$$\delta_S = 23.45\left(\frac{2\pi}{360}\right)\sin\left(\left(\frac{2\pi}{360}\right)0.986(J-80)\right) \text{ radians , and}$$

$$h_s = \left(\frac{2\pi}{360}\right)\left[15\left(12\text{-}\left(Z-\frac{\lambda}{15}\right)\right)\right] \text{ radians}.$$

4.2.2 AUTOMATIC WIND DATA ENTRY USING A SAM

ALOHA can be connected to a Station for Atmospheric Measurements (SAM) for direct wind measurements. Stability class can be derived from the wind speed and measured standard deviation in the wind direction, $\sigma_{\theta,m}$, in combination with user-entered surface roughness and solar radiation. The method used to estimate stability class was described by the U.S. Environmental Protection Agency (United States. Environmental Protection Agency 1987).

The method is based on the wind speed at 10m, and a **Surface Roughness Length**, z_0, equal to 15 cm. If the roughness length is different than 15 cm, the standard deviation in wind angle is adjusted to

$$\sigma_\theta = \sigma_{\theta,m}\left(\frac{z_0}{0.15}\right)^{0.2}.$$

An initial estimate of stability class is based on the standard deviation in wind direction measured at 10 meters.

Table 11. Initial estimate of stability class and standard deviation in wind direction.

Initial estimate of stability class	*Corrected σ_θ in degrees*
A	$22.5 \le \sigma_\theta$
B	$17.5 \le \sigma_\theta < 22.5$
C	$12.5 \le \sigma_\theta < 17.5$
D	$7.5 \le \sigma_\theta < 12.5$
E	$3.8 \le \sigma_\theta < 7.5$
F	$\sigma_\theta < 3.8$

If the measurement height is other than 10 meters, the table is adjusted. The lower bound to σ_θ on the table is multiplied by $(Z/10m)^{-P}$. The exponent is P = (0.06, 0.15, 0.17, 0.23, 0.38) for stability classes A through E, respectively.

The stability class is finally derived from the initial estimate and the wind speed measured at 10m. Nighttime is the period from 1 hour before sunset to 1 hour after sunrise.:

Table 12. Stability class for daytime and nighttime.

Daytime		
Initial Class	U_{10} (m s^{-1})	Final Class
A	$U_{10} < 3$	A
A	$3 < U_{10} < 4$	B
A	$4 \leq U_{10} < 6$	C
A	$6 \leq U_{10}$	D
B	$U_{10} < 4$	B
B	$4 \leq U_{10} < 6$	C
B	$6 \leq U_{10}$	D
C	$U_{10} < 6$	C
C	$6 \leq U_{10}$	D
D, E, F	any speed	D

Nighttime		
Initial Class	U_{10} (m s^{-1})	Final Class
A	$U_{10} < 2.9$	F
A	$2.9 \leq U_{10} < 3.6$	E
A	$3.6 \leq U_{10}$	D
B	$U_{10} < 2.4$	F
B	$2.4 \leq U_{10} < 3.0$	E
B	$3.0 \leq U_{10}$	D
C	$U_{10} < 2.4$	E
C	$2.4 \leq U_{10}$	D
D	any speed	D
E	$U_{10} < 5.0$	E
E	$5.0 \leq U_{10}$	D
F	$U_{10} < 3.0$	F
F	$3.0 \leq U_{10} < 5.0$	E
F	$5.0 \leq U_{10}$	D

4.2.3 WIND PROFILE

The air dispersion models used in ALOHA require the vertical wind-speed profile. A steady-state wind varies significantly with height near the surface. Dispersion in the alongwind direction is generated mostly by this vertical wind shear. ALOHA uses the entered wind speed and reference height along with atmospheric stability and ground roughness data to compute a wind profile. Wind profile formulations are based on the assumption that wind speed and direction, as well as all other atmospheric conditions, remain horizontally homogeneous and do not change during the duration of a release.

The wind profile is affected by the irregularities of the solid surface over which the air moves. Obstacles such as trees, bushes, even blades of grass have an impact on the vertical profile of the wind. The ALOHA user chooses ground roughness conditions by entering a numerical value for

ground roughness length, z_0 (m), or selecting one of three terrain conditions: Choosing Open Country sets the surface roughness to 0.03 m, Urban or Forest sets the surface roughness to 1 m, Open Water sets the surface roughness to a value based on the wind speed at 10 meters, U_{10} (m s^{1}):

$$z_0 = 0.0000026\,(U_{10})^{2.5}$$

The dispersions models in ALOHA use surface roughness lengths in a limited fashion. The Gaussian Model only distinguishes between large and small ground roughness, and the Heavy Gas model uses a roughness length of 0.10 m for all user-specified roughness lengths greater than 0.10 m.

In parts of the model, ALOHA approximates the wind profile within the surface sublayer using

$$U(z) = \frac{U_*}{k}\left[\ln\frac{z+z_0}{z_0} + \psi(\zeta)\right],$$

where

U_* is the friction wind velocity,

$U(z)$ is the mean wind at reference height *z*,

k is the von Kármán constant, taken to be 0.4,

z_0 is the ground roughness length, and

$\zeta = z/L$ is the non-dimensional height.

ALOHA uses the following empirical equations to relate the Obukhov length, *L*, to the surface roughness length under each Pasquill stability class:

$$L = \begin{cases} -11.4 z_0^{0.10} & \text{Class A,} \\ -26.0 z_0^{0.17} & \text{Class B,} \\ -123 z_0^{0.30} & \text{Class C,} \\ \infty & \text{Class D,} \\ 123 z_0^{0.30} & \text{Class E,} \\ 26.0 z_0^{0.17} & \text{Class F.} \end{cases}$$

The function $\psi(\zeta)$ depends on the sign of the dimensionless height. For unstable, neutral, and stable surface sublayers (Businger 1973), ALOHA uses empirical equations,

$$\psi(\zeta) = \begin{cases} \frac{2\ln(1+a)}{2} + \frac{\ln(1+a^2)}{2} - 2\arctan a + \frac{\pi}{a} & \zeta < 0, \\ 0 & \zeta = 0, \\ -4.7\zeta & \zeta > 0, \end{cases}$$

where

$$a = (1-15\zeta)^{1/4}.$$

In most cases, ALOHA uses a power function (Brutsaert 1982), rather than a logarithmic function, to describe the wind profile within the surface sublayer:

$$U_2 = U_1\left(\frac{z_2}{z_1}\right)^n.$$

The exponent n greatly affects heavy gas dispersion computations. DEGADIS matches the logarithmic profile for the given ambient conditions to estimate the exponent, n. For $z_0 = 15cm$ and Pasquill stability classes A to F, typical values of n are 0.109, 0.112, 0.120, 0.142, 0.203, 0.253.

4.3 GAUSSIAN MODEL FOR NEUTRALLY BUOYANT GASES

ALOHA's Gaussian dispersion model is intended to be used with vapor clouds that do not significantly affect the ambient air flow, and are not affected by gravity; they are considered passive pollutants.

The Gaussian model predicts that the concentration distribution of a steady-state release of neutrally buoyant gas will approach a Gaussian distribution with increasing down-wind distance. The parameters characterizing the distribution are based on empirical measurements. Increasing averaging times of the measurements also tend to drive the distribution to a Gaussian shape, as well as widen the spatial distribution. The actual concentration distribution from a release can vary significantly from Gaussian at any single instant in time.

The method used in ALOHA accommodates instantaneous, continuous, and time-dependent releases of finite duration up to one hour. An instantaneous release is modeled as a single one-minute steady-state release which gives rise to a single cloud. A continuous release is modeled as a single one-hour steady-state release which gives rise to a single cloud.

A time-dependent release is modeled as series of five finite-duration steady-state releases; each giving rise to a cloud that does not interact with the other clouds. The concentration at a point in space and time is found by summing the contributions from each cloud.

The model used to describe the dispersion of each cloud is based on a Gaussian dispersion model developed by Palazzi (Palazzi et al. 1982) that describes the behavior of steady state releases of short duration. This model is described as

$$C(x,y,z,t)=\begin{cases}\dfrac{\chi}{2}\left[\operatorname{erf}\left(\dfrac{x}{\sigma_x\sqrt{2}}\right)-\operatorname{erf}\left(\dfrac{(x-Ut)}{\sigma_x\sqrt{2}}\right)\right] & (t\le t_r),\\ \dfrac{\chi}{2}\left[\operatorname{erf}\left(\dfrac{x\text{-}U\left(t-t_r\right)}{\sigma_x\sqrt{2}}\right)-\operatorname{erf}\left(\dfrac{x-Ut}{\sigma_x\sqrt{2}}\right)\right] & \left(t_r<t<\infty\right),\end{cases}$$

where

σ_x, σ_y, and σ_z are the dispersion parameters,

t_r is the duration of the release.

The term χ represents a well-known Gaussian distribution from a continuous steady-state point source (Hanna et al. 1982),

$$\chi(x,y,z,t)=\left(\frac{Q(t)}{U}\right)g_y(x,y)\,g_z(x,z),$$

where

$$g_y(x,y)=\frac{1}{\sqrt{2\pi}\sigma_y(x)}\exp\left[-\frac{1}{2}\left(\frac{y}{\sigma_y(x)}\right)^2\right],$$

and, when no inversion is present,

$$g_z(x,z)=\frac{1}{\sqrt{2\pi}\sigma_z(x)}\left\{\exp\left[-\frac{1}{2}\left(\frac{z-h_s}{\sigma_z(x)}\right)^2\right]+\exp\left[-\frac{1}{2}\left(\frac{z+h_s}{\sigma_z(x)}\right)^2\right]\right\},$$

Where h_s is the height of the release.

The presence of an inversion can have a significant effect on the vertical diffusion of the cloud. When a layer of unstable air at the ground lies beneath a layer of stable air, the interface acts to contain the pollutant cloud. The effect of an inversion can be quite complex and simplifications

were required in ALOHA. As a conservative approximation, ALOHA models the interface between the stable and unstable air as impervious to the transport of the pollutant. The ground and the inversion act as a pair of reflecting surfaces for the pollutant cloud. Note that ALOHA only accommodates situations where the inversion height, h_i, is above the height of the release, h_s. The form of $g_z(x,z)$ represents the repeated reflection, up to J=5, of the pollutant cloud, and is described as

$$g_z(z,x) = (2\pi)^{-1/2}\left(\frac{1}{\sigma_z}\right)\left\{\exp\left[-\frac{1}{2}\left(\frac{(z-h_s)^2}{\sigma_z^2(x)}\right)\right] + \exp\left[-\frac{1}{2}\left(\frac{(z+h_s)^2}{\sigma_z^2(x)}\right)\right]\right\} +$$

$$\sum_{n=1}^{J}\left\{\begin{array}{l}\exp\left[-\frac{1}{2}\left(\frac{(z-2nh_i-h_s)^2}{\sigma_z^2(x)}\right)\right] + \exp\left[-\frac{1}{2}\left(\frac{(z+2nh_i-h_s)^2}{\sigma_z^2(x)}\right)\right] \\ + \exp\left[-\frac{1}{2}\left(\frac{(z-2nh_i+h_s)^2}{\sigma_z^2(x)}\right)\right] + \exp\left[-\frac{1}{2}\left(\frac{(z+2nh_i+h_s)^2}{\sigma_z^2(x)}\right)\right]\end{array}\right\},$$

where h_i is the height of the inversion.

Far downwind, the repeated reflections of the cloud tend to produce a uniform concentration beneath the inversion. ALOHA approximates the vertical distribution as homogenous at distances downwind such that $\sigma_z(x) \geq 2h_i$.

4.3.1 DETERMINATION OF DISPERSION PARAMETERS

The concentration distribution described above is a Gaussian distribution parameterized by three empirical dispersion parameters. These are the standard deviations of the Gaussian distribution: $\sigma_x, \sigma_y, and\ \sigma_z$. The dispersion parameters depend upon the stability class, and in some cases the surface roughness. They also depend upon the averaging times associated with their measurement.

Briggs developed formulas for estimating σ_y and σ_z for each of the Pasquill-Gifford-Turner stability classes, and for Urban (large surface roughness) and Rural (small surface roughness) conditions (Briggs 1973, Hanna et al. 1982):

$$\sigma_y(x) = \frac{s_{y1}x}{\sqrt{1+s_{y2}x}} \quad \text{and} \quad \sigma_z(x) = s_{z1}x(1+s_{z2}x)^{s_{z3}}.$$

The values of the parameters are presented as a function of atmospheric stability and roughness in Table 13.

Briggs analysis employed only two surface roughness classifications: Urban corresponds to large ground roughness, or Rural which corresponds to small surface roughness. If the user-specified ground roughness is less than 20 cm, Rural is selected, otherwise Urban is selected.

Averaging times varied for the experiments used to determine dispersion parameters; however, Briggs did not adjust the coefficients used to estimate σ_y to account for the different averaging times associated with the data sets from which they were derived (Blewitt 1990). The rural coefficients were derived from data averaged over 3 minutes, and the urban coefficients were derived from data averaged over 1 hour. When the coefficients are corrected for this difference, the formulas produce similar curves (Blewitt 1990). For this reason, ALOHA uses only the rural coefficients based on 3-minute averaging times to estimate σ_y under all surface roughness conditions.

To estimate σ_z, Briggs derived a set of analytical solutions from two different experiments. Data used for values of σ_z greater than 100 m relfect a 1-hour averaging time, while data used for smaller values of the σ_z reflect averaging times of 10 to 15 minutes (Briggs 1991). There is no definitive averaging time associated with this parameter, and we do not expect σ_z to be strongly dependence on averaging time.

To estimate σ_x, the standard deviation function in the alongwind direction, ALOHA uses the following formula, which is based on Beals (Beals 1971) and is also used in the heavy gas model DEGADIS (Havens and Spicer 1985). Beals made no reference to the associated averaging times for σ_x, and we do not expect σ_x to be strongly dependent on averaging time. The formula is shown as

$$\sigma_x\left(x_0\right) = s_{x1} x_0^{s_{x2}}.$$

Table 13. Values for the coefficients used to estimate the dispersion parameters.

		Stability Class					
Roughness	**Coefficient**	**A**	**B**	**C**	**D**	**E**	**F**
Both	s_{x1}	0.02	0.02	0.02	0.04	0.17	0.17
	s_{x2}	1.22	1.22	1.22	1.14	0.97	0.97
	s_{y1}	0.22	0.16	0.11	0.08	0.06	0.04
	s_{y2}	0.0001	0.0001	0.0001	0.0001	0.0001	0.0001
Small Surface Roughness (Rural)	s_{z1}	0.2	0.12	0.08	0.06	0.03	0.016
	s_{z2}	0	0	0.0002	0.0015	0.0003	0.0003
	s_{z3}	0	0	-0.5	-0.5	-1	-1
Large Surface Roughness (Urban)	s_{z1}	0.24	0.24	0.2	0.14	0.08	0.08
	s_{z2}	0.001	0.001	0	0.0003	0.0015	0.0015
	s_{z3}	0.5	0.5	0	-0.5	-0.5	-0.5

Note: An incorrect value of 0.00015 for s_{z2} was presented in Briggs (1973) and many later references. ALOHA uses the correct value, 0.0015.

4.4 HEAVY GAS MODEL FOR DENSE GASES

The Heavy Gas dispersion calculations used in ALOHA are based on the DEGADIS model (Havens and Spicer 1985, Spicer and Havens 1989). DEGADIS, in turn, is an adaptation of the Shell HEGADIS model described by Colenbrander (Colenbrander 1980, Colenbrander and Puttock 1983); DEGADIS also incorporates some techniques used by van Ulden (van Ulden 1974, 1983). DEGADIS was selected as the basis for ALOHA's dense gas computations because of its general acceptance and the extensive testing that was carried out by its authors.

Some simplifications were introduced into ALOHA-DEGADIS, making it different from the DEGADIS model. ALOHA-DEGADIS is limited to releases at ground level, and does not account for the initial momentum from a jet release. Some of the numerical methods used in ALOHA-DEGADIS have been simplified compared to those used in DEGADIS. The ambient air pressure used in ALOHA is independent of position and time. The pollutant and air are assumed to behave as non-interacting ideal gases.

The method for handling releases that vary with time is unique to ALOHA. DEGADIS is designed to model steady-state releases, while ALOHA is designed to model time-dependent releases. The ALOHA-DEGADIS model is essentially the DEGADIS steady-state plume model that has been adapted to handle time-varying sources. For any non-instantaneous sources in ALOHA, the model generates a five-step release; each step is a finite-duration steady-state release. The Heavy Gas model generates infinite-duration steady-state plumes for each of these sources. A composite time-varying cloud is created by adding together pieces of the five steady-state plumes. The pieces start

as steady-state plumes ten meters in length. Each piece is converted into a Gaussian in the downwind direction, conserving mass, but maintaining its vertical and horizontal dimensions. The pieces are summed to create the time-varying cloud. The Guassian dispersion parameter used, σ_x, is the same as that used in the Gaussian dispersion model (Beals 1971).

ALOHA-DEGADIS has beenverified by comparisons to field experiments, the original DEGADIS model, and other reference models. As part of the verification process, the authors of both models reviewed each model's code and computations line by line (Havens 1990).

Estimates made by ALOHA-DEGADIS and DEGADIS for a series of release scenarios were also compared. Using a fractional factorial experimental design (Cochran and Cox 1957), a set of 24 test scenarios was prepared. Eight DEGADIS input variables—stability class, wind speed, spill size, release duration, gas density, ground roughness, chemical-ground temperature difference, the coefficients of the equation of state, and level of concern—were varied in the 24 scenarios in order to span the expected variability within model parameters. We believe that these factors are the most important influences on concentration estimates made by DEGADIS.

For the 24 cases, the correlation between the estimates of concentration and downwind distance made by the two models was 0.997. For steady-state, continuous release cases, ALOHA-DEGADIS tended to predict a longer distance than was predicted by the full DEGADIS model. ALOHA-DEGADIS threat zones averaged 10% longer than those predicted by DEGADIS. For short-term releases, the arrival time of the peak concentration at a given location downwind and the maximum value of the peak were also examined. Arrival times predicted by ALOHA-DEGADIS were slightly later than those predicted by DEGADIS, although the correlation between estimates made by each model was 1.0. ALOHA-DEGADIS predicted downwind movement of gas clouds to average about 9% slower than the travel rate predicted by DEGADIS. ALOHA-DEGADIS predicted maximum concentrations that exceeded DEGADIS estimates by an average of 8%. The correlation between maximum concentration estimates made by the two models was 0.994%.

These results demonstrate that the ALOHA-DEGADIS model is consistently slightly more conservative than DEGADIS. It can be expected to produce peak concentration estimates for a given point that are, on average, about 10% greater than estimates made by the full DEGADIS model.

4.4.1 CRITERIA FOR USE OF THE HEAVY GAS MODEL

The ALOHA Heavy Gas model is designed to account for the gravitational effects on pollutant clouds with densities significantly different than air. Gravitational effects can be insignificant for dense pollutants if the dispersion is dominated by the wind or thermal convection in the atmosphere, or the evaporative flux from a pool is small. The Heavy Gas model can still be used with these clouds, but the Gaussian Model is preferred. The Gaussian model is also recommended when the pollutant cloud is less dense than air.

In its default mode, ALOHA incorporates a decision algorithm to choose between the Heavy Gas and Gaussian models. ALOHA uses the critical Richardson's Number (also called the friction Richardson's Number), Ri_C, as the criterion for distinguishing between passive or non-passive dispersion. When Ri_C is less than 1, ALOHA considers the gas to be passive and, unless the user

overrides this decision, ALOHA computes dispersion using the Gaussian dispersion model (Spicer and Havens 1989).

The critical Richardson number depends upon the density of the pollutant, the wind speed, and the release rate,

$$Ri_c = \frac{H * \hat{g}}{U_*^2},$$

where the reduced gravity is

$$\hat{g} = \frac{g(\rho - \rho_a)}{\rho_a},$$

ρ is the density of the chemical,
ρ_a is the density of the ambient air,
g is the acceleration of gravity,
U_* is the friction velocity of the wind, and
H is the characteristic dimension of the source.

For instantaneous releases, H is the characteristic height of the source,

$$H = V_0 \big/ A_0,$$

where V_0 is the volume of the release and A_0 is the area of the source.

For puddle sources, the characteristic height of the source is related to the release rate and diameter of the puddle and is found using

$$H = \frac{E}{\rho U_{10} D},$$

where
E is the mass evaporation rate (kg s^{-1}),
D is the diameter of the puddle, and
U_{10} is the wind speed at 10 meters.

For continuous or semi-continuous sources other than the puddle source, the characteristic dimension is

$$H = \sqrt{\frac{E\pi}{4\rho U_{10}}}.$$

4.4.2 CONCEPTUAL MODEL

Havens and Spicer (Havens and Spicer 1985) described three stages in a heavy gas release. This is the conceptual model used in DEGADIS and ALOHA-DEGADIS.

1. Buoyancy-Dominated Dispersion. Near the point of a release, buoyancy forces, inertial forces, and ambient air motions all affect cloud development. Immediately after it is released, a heavy cloud "slumps" over the ground. The rapidly spreading cloud forces itself under the ambient atmospheric boundary layer. As it does so, shear at the ground and at the top of the cloud creates a vortex ring at the forward edge of the cloud (Britter 1989). During this initial spreading, the cloud entrains approximately 10 times its original mass of ambient air. That is, the density ratio is reduced by a factor of 10. By the end of this stage, a thin **blanket** of gas has formed. The blanket constitutes the secondary source.

The buoyancy-dominated stage evolves through three overlapping sub-stages:

(i) During the *slumping phase*, which lasts only a few seconds, strong, buoyancy-dependent spreading forces are balanced by counterflow of the ambient fluid.

(ii) During the *buoyancy-inertial phase*, buoyancy spreading forces are balanced by inertial forces. Concentrations within the cloud are greatly diluted as the spreading "head" of the cloud entrains ambient fluid.

(iii) During the *viscous phase*, buoyancy forces are balanced by viscous forces. Turbulent mixing is suppressed, and the dilution rate slows.

2. Stably Stratified Shear Flow. In this region, buoyancy forces and ambient air flow determine the cloud development, acting to produce a stably stratified cloud embedded in the mean wind flow. The cloud remains thin and spreads laterally as it is advected downwind. The stable density profile in the cloud suppresses turbulence, and turbulent fluctuations in the cloud are characteristically below-ambient levels. Air is entrained into the spreading cloud primarily through its top as well as along its edges.

3. Passive Turbulent Dispersion. The cloud continues to be diluted until its density only slightly exceeds the density of the air. The small remaining density difference only negligibly affects cloud dispersion, and natural levels of turbulence return. The gas becomes a passive contaminant.

4.4.3 SECONDARY SOURCE IN ALOHA

ALOHA does not explicitly model the buoyancy-dominated dispersion that leads to the formation of a heavy gas blanket, also called the Secondary Source. Instead, it uses a simplified method to estimate the blanket dimensions.

Four source types are described in Chapter 2: direct release, tank release, pipeline release, and evaporating puddle. For heavy gas modeling, these are referred to as the **Primary Sources.** The Primary Source is generally time dependent and approximated as a series of five finite-duration steady-state sources.

The heavy gas model is fundamentally a steady-state plume model, while the Primary Sources are generally time-dependent. To approximate the time-dependence of the plume, ALOHA generates steady-state plumes based on the five time steps of the Primary Source, treating each as a time-independent steady-state source. Time dependence is later introduced by combining the time-independent plumes.

The buoyancy-dominated stage of a heavy gas release generates a "blanket" of dense gas which is centered on the location of the Primary Source and does not move with the ambient air flow. The Primary Source feeds this blanket at a constant rate, while the uptake and transport of gas from the top of the blanket removes gas from the blanket. The atmospheric uptake rate is proportional to the area of the blanket, so the blanket reaches its steady-state size when the atmospheric uptake rate equals the Primary Source. The blanket is assumed to be circular.

Most of the Primary Sources in ALOHA are point sources; however, the evaporating puddle has a defined area. If the area of the evaporating puddle is greater than the steady-state area of the heavy gas blanket, the area of the blanket is set equal to the puddle area.

The total mass of the developing blanket is

$$M_b(t) = A(t)H_b(t)\rho(t),$$

where
$A(t)$ is the area of the blanket,
$H_b(t)$ is the blanket height, and
$\rho(t)$ is the overall mean density of the blanket.
$M_b(t), A(t), H_b(t), \rho(t)$ are unknowns.

The rate of change in the blanket mass depends on the entrainment of air and contaminant into the cloud,

$$\frac{dM_b}{\mathrm{d}t} = \frac{E(t)}{w_{c,p}(t)} + Q_a(t) - A(t)\left[\frac{Q_{*\max}(t)}{w_c(t)}\right],$$

where
$E(t)$ is the contaminant evolution rate from the Primary Source (kg s^{-1}),
$w_{c,p}(t)$ is the contaminant mass fraction in the primary source,
$Q_a(t)$ is the entrainment rate into the air above the blanket (kg s^{-1}),
$Q_{*\max}$ is the maximum mass flux into the air from the blanket (kg $s^{-1}m^{-2}$), and
$w_c(t)$ is the mass fraction of contaminant in the developing cloud.
$Q_a(t)$, $Q_{*\max}(t)$, and $w_c(t)$ are unknowns.

The terms $E(t)$ and $w_{c.p}(t)$ depend on the primary source and are provided as external parameters.

In the final phases of the developing cloud, (humid) air entrainment is primarily through the top, and its rate is given by

$$Q_a(t) = \frac{\left(2\pi R_b(t) H_b(t) \rho_a(t) (\varepsilon u_f(t)\right)}{\left(\hat{g}(t) H_b(t) / u_f(t)^2\right)},$$

where
$\hat{g}$ is the reduced gravity defined in a previous section,
$R_b(t)$ is the radius of the blanket,
ε is the entrainment rate coefficient at the front of the cloud, and
u_f is the rate of advance of the cloud front, $u_f(t) = dR_b(t)/dt$.

The total mass of contaminant in the source blanket is

$$M_c(t) = w_c(t) 2\pi R_b(t)^2 H_b(t) \rho(t) = w_c(t) M_b(t),$$

and its rate of change is

$$\frac{\mathrm{d}M_c(t)}{\mathrm{d}t} = E(t) - A(t) Q_{*\max}(t).$$

The amount of air in the source blanket is

$$M_a(t) = (1 - w_c(t)) 2A(t) H_b(t) \rho(t) = (1 - w_c(t)) M_b(t),$$

and its rate of change is

$$\frac{\mathrm{d}M_a(t)}{\mathrm{d}t} = \frac{E(t)}{w_{c,p^{(t)}}} \left[\frac{1 - w_{c,p}(t)}{1 + q_a} \right] + \frac{Q_a(t)}{1 + q_a} - w_a(t) A(t) \frac{Q_{*\max}(t)}{w_c(t)},$$

where q_a is the absolute humidity.

The total energy in the cloud is

$$U_b(t) = \pi h_b(t) R_b(t)^2 H_b(t) \rho(t),$$

where
U_b is the total energy in the cloud and
h_b is the mean enthalpy (J kg^{-1}) for the blanket.

The rate of change is

$$\frac{\mathrm{d}U_b(t)}{\mathrm{d}t} = \frac{h_s(t)E(t)}{w_{c,p}(t)} + h_a Q_a(t) - \pi h_b(t) R_b(t)^2 \left[\frac{Q_{*\max}(t)}{w_c(t)}\right] + \pi R_b(t)^2 F_{HS}(t),$$

where

h_s is the enthalpy of the primary source,

h_a is the enthalpy of air, and

$F_{HS}(t)$ is the surface heat flux.

These relationships are solved simultaneously to obtain the steady state limit of the blanket variables.

4.4.4 STABLY STRATIFIED SHEAR FLOW AND PASSIVE DIFFUSION STAGES

The heavy gas dispersion model in DEGADIS is almost identical to the similarity model proposed by Colenbrander (Colenbrander 1980).

Air flow over the blanket creates a plume of heavy gas. To simplify computation, the cylindrical blanket is treated as a square prism of equal volume and height. The plume is assumed to be composed of (i) a horizontally homogeneous core of width 2b that has vertical dispersion, and (ii) Gaussian-shaped edges. As the plume transitions from stably stratified shear flow to passive turbulent diffusion, the width of the homogeneous core goes to zero. The following equation for the concentration of the pollutant is applicable to both regions:

$$c(x,y,z) = \begin{cases} c_c(x)\exp\left(-\dfrac{|y|-b(x)}{S_y(x)}\right)^2 - \left(\dfrac{z}{Sz}\right)^{1+n} & |y| > b(x), \\ c_c(x)\exp\left(-\left(\dfrac{z}{S_z}\right)^{1+n}\right) & |y| \le b(x). \end{cases}$$

Four variables are functions of x and must be computed for each downwind step:

$c_c(x)$ is the centerline ground-level concentration (ppm),

$S_y(x)$ is the lateral dispersion parameter (m),

$S_z(x)$ is the vertical dispersion parameter (m), and

b is the half-width of the homogeneous core section (m).

The dispersion parameters are based on measurements. We do not expect the vertical dispersion parameter to be strongly dependent on the averaging times used in its measurement. However, the horizontal dispersion does have a dependence on averaging time; it is thought to scale with the averaging time raised to the 0.2 power. ALOHA-DEGADIS adjusts the horizontal dispersion parameter to correspond to an averaging time of 5 minutes for toxic clouds, and 10 seconds for flammable clouds.

In the discussion to follow, a coupled set of empirical parametric equations will be presented. This set of equations must be solved simultaneously at each step in the x direction.

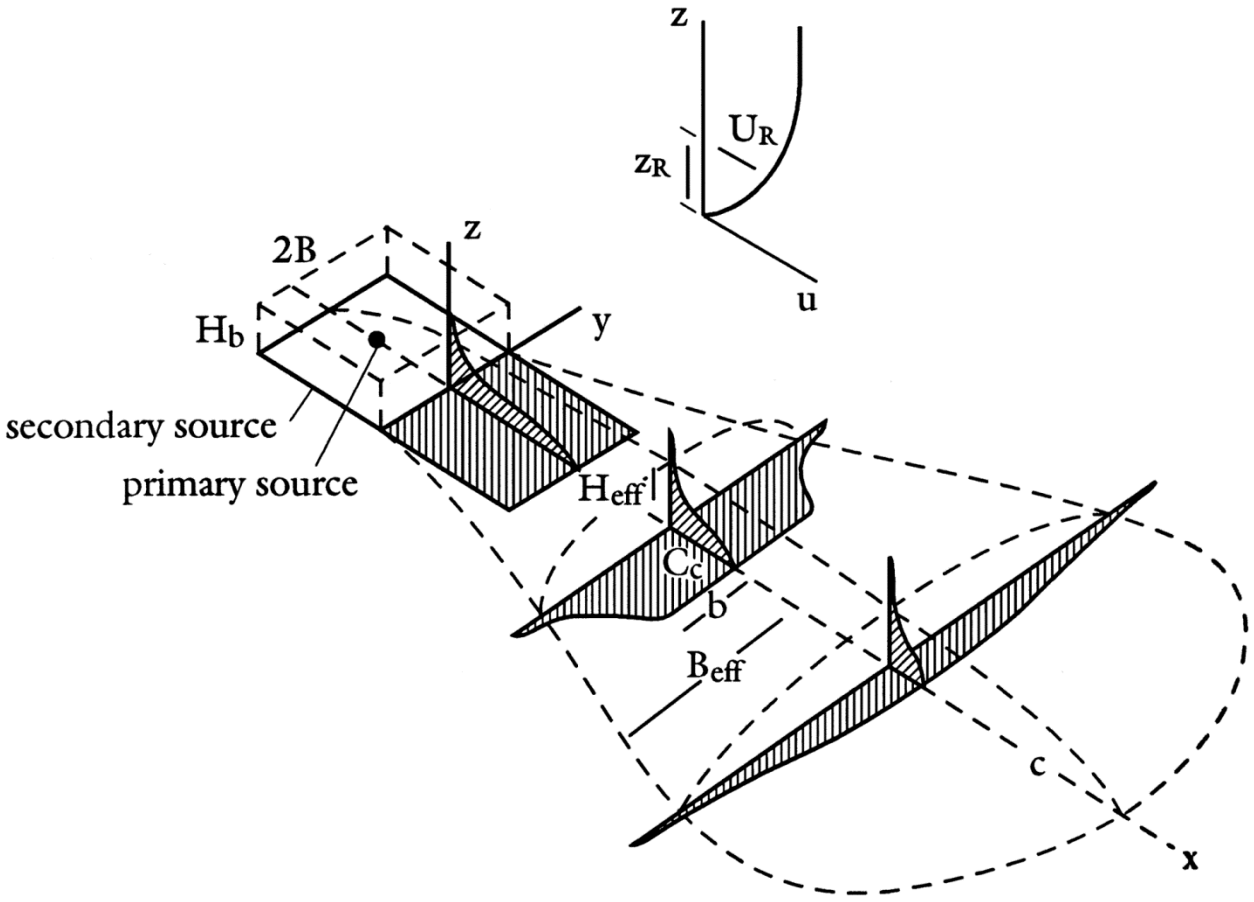

Figure 2. The plume model proposed by (Colenbrander 1980).

4.4.4.1 The Effective Cloud Width, Height, and Velocity

Empirical formulations for the plume/cloud dispersal require a cloud height parameter. The **effective cloud height**, H_{eff}, is based on the centerline concentration of contaminant in the form

$$H_{eff}(x) = \frac{1}{c_c(x)} \int_0^\infty c(x,0,z)dz\,.$$

The effective cloud height is

$$H_{eff}(x) = \frac{S_z(x)}{1+n}\,\Gamma\left(\frac{1}{1+n}\right),$$

where Γ $(1/(1 + n))$ is the gamma function. This term will appear several times in the development below and will be written simply as Γ.

We define an **effective cloud width** by the sum of the constant concentration central core, b(x) and the tail-off region on each side as

$$B_{eff}(x) = b(x) + \frac{\sqrt{\pi}}{2} S_y(x).$$

The lateral spread of the cloud is modeled by a Froude number representation as

$$\frac{\mathrm{d}B_{eff}}{\mathrm{d}x} = C_E \Gamma \left(\frac{Z_R}{S_z(x)} \right)^n \left[\frac{\hat{g} H_{eff}(x)}{U_R^2} \right]^{1/2},$$

where C_E is a constant.

At some x downwind, $b(x) \to 0$ and the cloud width is defined by $S_y(x)$. The cloud initially spreads under the influence of the reduced gravity, $\hat{g}$, then as the cloud is diluted and $S_z(x)$ grows, the core area diminishes to zero, at which point the heavy gas effects cease.

The **effective cloud velocity** in the plume is the concentration-weighted mean of the wind speed,

$$U_{eff}(x) = \frac{\int_0^\infty c(x,0,z) U \mathrm{d}z}{\int c(x,0,z) \mathrm{d}z} = \left(\frac{S_z(x)}{Z_R} \right)^n \frac{U_R}{\Gamma},$$

where U_R is the wind speed at reference height Z_R.

4.4.4.2 Bulk Richardson Number

The **Bulk Richardson Number** is

$$\mathrm{Ri}_*(x) = \frac{\hat{g}(x) H_{eff}(x)}{U_*^2}.$$

Experiments show that in continuous releases the plume has well-defined sharp edges when $\mathrm{Ri}_* > 1$ and lateral concentration profile approaches a Gaussian shape when $\mathrm{Ri}_* < 1$.

4.4.4.3 Corrections to Ri$_*$ for Heat Flux

When the surface temperature under the plume, T_S, is greater than the mean temperature of the cloud, $T_c(x)$, a positive heat flux reduces the cloud stability. In this case, Ri$_*$ is corrected in the form

$$\mathrm{Ri}_*'(x) = \mathrm{Ri}_*(x)\left(U_*/\sigma_w\right)^2,$$

where σ_W is the root-mean-square (rms) vertical velocity at the top of the gas cloud. The ratio (σ_w/U_*) to the top of the cloud is estimated by

$$\frac{\sigma_w}{U_*} = \left(1+ \mathrm{Ri}_T^{2/3}\right)^{1/2},$$

where the bulk temperature Richardson Number, Ri_T ,is given by

$$\mathrm{Ri}_T = g\left[\frac{T_s - T_c}{T_c}\right]\frac{H_{eff}}{U_* U_R}\left[\frac{Z_R}{H_{eff}}\right]^n.$$

This equation introduces a new unknown, the cloud temperature, $T_c(x)$. A cloud energy balance must be added to the equation set in order to estimate this term.

4.4.4.4 Heavy Gas Dispersion Coefficients

Two-dimensional diffusion equations represent a balance between the downwind gradient in concentration and either the vertical or the lateral turbulent diffusion. By separation of variables

$$U\frac{\partial c(x,y,z)}{\partial x} = \frac{\partial}{\partial z}\left(K_z\frac{\partial c}{\partial z}\right) \text{and}$$

$$U\frac{\partial c(x,y,z)}{\partial x} = \frac{\partial}{\partial y}\left(K_y\frac{\partial c}{\partial y}\right).$$

The equations are solved using the power-law approximation for the wind profile described earlier in this chapter, and the empirical approximations of

$$K_z(x,z) = \frac{kU_* z}{\phi\left(\mathrm{Ri}_*'(x)\right)} \text{and}$$

$$K_y(x) = K_0 U B_{eff}(x)^{\gamma 1},$$

where $\gamma 1$ is a constant, K_0, is a dimensionless constant $\left(=n^{(1-\gamma 1)}\right)$ and $\phi\left(\mathrm{Ri}'_*\right)$ is a stability factor given by

$$\phi\left(\mathrm{Ri}'_*\right)=0.88+\left(0.099\,\mathrm{Ri}'^{1.04}_*\right)+\left(1.4*10^{-25}\ \mathrm{Ri}'^{5.7}_*\right)\quad \mathrm{Ri}'\geq 0\,.$$

The previous equations are solved to yield the similarity form of the dispersion equation in the x-z plane:

$$\frac{\mathrm{d}}{\mathrm{d}x}\left[\left(\frac{U_R Z_R}{1+n}\right)\left(\frac{S_z(x)}{Z_R}\right)^{1+n}\right]=\frac{kU_*\left(1+n\right)}{\phi\left(\mathrm{Ri}'_*\right)}.$$

4.4.4.5 Mass and Energy Balance

The mean density of the cloud gas mixture depends on the $c_c\left(x\right)$ and temperature, T_c. These are approximated from a combined mass and energy balance for a differential slice with thickness dx, width of B_{eff}, and height H_{eff}.

The mass balance at x is given by $\left(\rho U_{eff} H_{eff} B_{eff}\right)$ and

$$\frac{\mathrm{d}}{\mathrm{d}x}\left[\rho U_{eff} H_{eff} B_{eff}\right]=\frac{\rho_a k\sigma_w\left(1+n\right)}{\phi\left(\mathrm{Ri}'_*\left(x\right)\right)}B_{eff}\left(x\right).$$

When the surface temperature is greater than the cloud temperature, then Ri∗ is corrected and the cloud temperature is a new dependent variable, $T_C(x)$. The temperature of the cloud will change as heat is added to the cloud by flux of sensible heat from the ground, F_H. The added energy density of the cloud, D_h, in (J kg^{-1}) is computed from

$$D_h(x)=c_{pg}(x)\left(T_c(x)-T_c(0)\right).$$

The energy budget for a transverse slice of the cloud is

$$\frac{\mathrm{d}}{\mathrm{d}x}\left[D_h\rho U_{eff} H_{eff} B_{eff}\right]=F_H\ B_{eff}\,/\delta_L\ ,$$

where F_H is the surface heat flux under the cloud, and δ_L is an empirical constant.

When the core width b = 0, the energy balance becomes

$$\frac{\mathrm{d}}{\mathrm{d}x}\left[D_h\rho U_{eff} H_{eff}\right]=F_H\,/\,\delta_L\,.$$

The steady-plumes generated by the Heavy Gas model are combined to create a time-dependent cloud, as described in the General Comments section above.

4.5 THREAT ZONE

ALOHA's threat zone represents the area within which the ground-level gas concentration exceeds the level of concern at any time.

4.5.1 ESTIMATING MAXIMUM CONCENTRATION

The concentration of the pollutant is a function of both location and time. In order to generate a threat zone, ALOHA calculates the peak concentration as a function of time for all points in space. It is important to note that this is not a true peak in the concentration since the concentrations predicted by ALOHA are time-averaged over different time intervals, depending upon the dispersion model employed. Implicit averaging times within the dispersion models vary.

The maximum concentration function M(x,y) for any point (x,y) is defined to be the maximum over all time of concentration at that point, and is given by

$$M(x,y) = \max_{-\infty \le t \le \infty} \left[C(x,y,t) \right].$$

ALOHA implements this function as follows. First, it identifies the source step associated with the highest release rate, and finds t_m (s), the time corresponding to the midpoint of that source step. It then finds t_0 (s), the time at which the cloud associated with that source step is centered at the point (x,0) as

$$t_0 = t_m + \frac{x}{u}.$$

ALOHA initially guesses the maximum concentration at (x,y) to be C(x,y,t_0). To test this, it compares the value of C(x,y,t_0) to C(x,y,t_0±30). If one of these values is larger, it compares concentrations in that direction using 30-second intervals for as long as concentration continues to increase.

4.5.2 DRAWING THE THREAT ZONE

The threat zone contour runs through points where the maximum concentration equals the LOC. At points within the threat zone, the maximum concentration function exceeds the LOC.

ALOHA constructs the threat zone contour in two steps. First, it performs a binary search of the maximum concentration function to find x_l, the downwind distance to the LOC (m). For a puddle source, ALOHA performs a second binary search to find the off-axis distances to the LOC from nine points equally spaced along the x-axis at distances 0, $x_l/8$, $2x_l/8$, $3x_l/8$...x_l. In the cases of point sources, ALOHA finds these off-axis distances using

$$y = \sigma_y \left(2 \log \left(\frac{M(x,0)}{LOC} \right) \right)^{1/2},$$

where x is the distance of each of the nine points along the x-axis. The threat zone contour runs through each of the (x,y) points found by this method. ALOHA uses a Bezier fit to connect these points by smooth curves.

4.5.3 CONFIDENCE CONTOURS

Uncertainties in the average wind direction are represented on the threat zone graph as confidence lines. The axis of the threat zone is rotated through an angle on either side of the nominal wind direction and the contour of the rotated threat zone is drawn. The angle, α, is based on the width of the Guassian plume at a distance 5 minutes downwind of the source,

$$\alpha = \arctan \left(\frac{2\sigma_y}{300 U_3} \right),$$

where U_3 is the wind speed at 3 meters (m s^{-1}).

4.6 INDOOR AIR CONCENTRATION

It is generally recognized that a well-insulated house or building provides excellent protection against a toxic cloud of finite time duration (Wilson 1987). Assuming the infiltration rate is small and that the air inside is always well-mixed, the building acts like a low-pass filter and an electrical R-C filtering circuit offers an excellent analog.

The infiltration time constant is the time required after a step-increase in the outside concentration of a gas for the concentration inside to reach 63% of the step difference. This number can vary from 1 to 0.1 hours depending on the building tightness, the wind, and the inside-outside temperature difference. The wind blowing against a building creates pressure differences and these drive infiltration and exfiltration depending on the direction of the pressure gradient. Temperature differences create a pressure gradient and thus enhance the infiltration process.

Because of the extreme variability in weather and building types, ALOHA must make some broad generalizations. Sherman (Sherman 1980, Sherman, Wilson, and Keil 1984) studied 196 houses and found that an effective leakage area is 0.00059 times the area of the house. ALOHA uses this figure and assigns an average house floor area of 160 m^2 (1722 ft^2). An average building ceiling height of

2.5 m is taken for a single-story house and 5m is used for a two-story building. A reasonable approximation of inside temperature is 20°C. It is assumed that all leakage occurs evenly over the structure and that there is no difference between floor and ceiling leakage.

We assume that the outside and inside concentrations are uniform and that environmental conditions are stationary in time. The balance of inflow and outflow of the chemical is

$$\frac{dc_i(t)}{dt} = \left(c_o(t) - c_i(t)\right) / \tau_E ,$$

where

$C_i(t)$ is the inside concentration,

$C_o(t)$ is the outside concentration, and

τ_E is the infiltration time constant.

The infiltration time constant can be specified by the user during setup. If not specified, it is approximated using a method based on the work of Sherman (Sherman 1980). The infiltration time constant is assumed to be proportional to the square root of the pressure differential between inside and outside, which in turn are dependent upon wind loading and temperature differences (stack effect). The infiltration time constant is

$$\tau_E = \left(\frac{V_S^2}{Q_S^2 + Q_W^2} \right)^{1/2} ,$$

where V_s is the total volume of the building.

The temperature-induced volume inflow rate depends on the absolute value of the temperature difference, ΔT (Grimsrud, Sherman, and Sonderegger 1983), and is described as

$$Q_s = A_e f_s \sqrt{|\Delta T|} ,$$

where

A_E is the effective leakage area = 0.00059x (floor area of the building).

The simplified stack parameter is

$$f_s = \frac{1 + R/2}{3} \sqrt{\frac{gH_S}{T_i}} ,$$

where

R is the ratio of vertical to total leakage set equal to 0.5,

H_S is the structure height, and

T_i is the uniform internal temperature.

The infiltration from wind loading is dependent upon the wind speed at the building height, U_H, and the sheltering of the building, and is given by

$$Q_w = A_e C_{sh} (1 - R)^{1/3} U_H ,$$

where

$$C_{sh} = \begin{cases} 0.24 \text{ sheltered} \\ 0.32 \text{ unsheltered} \end{cases} .$$

5 MODELS FOR CALCULATING BLAST EFFECTS FROM VAPOR CLOUD EXPLOSIONS

5.1 BACKGROUND

As an airborne chemical travels downwind, it mixes with air. A cloud containing a flammable chemical within its flammability limits can ignite if it encounters a spark, flame, or other ignition source. The combustion reaction can propagate away from the source by one of two mechanisms: Deflagration reactions propagate by means of diffusion of reactive species through the cloud. Detonation reactions propagate through a reactive fuel-air mixture by means of a pressure wave that travels at the local speed of sound. Deflagrations propagate more slowly than detonations; however, in either case, the reaction can cause temperatures and pressures within the cloud to increase dramatically. Both detonations and deflagrations can generate pressure waves with sharp onsets and significant overpressures; a pressure wave capable of causing damage to individuals or structures is called a blast wave in ALOHA.

Most vapor cloud combustions are deflagrations that propagate slowly and do not produce blast waves; these are usually referred to as flash fires. For some highly reactive chemicals, the flame speed (the propagation speed) within part of the cloud is accelerated by turbulence caused by obstacles or confinement resulting in a fast deflagration or transition to detonation; either is referred to as an explosion. These events can generate blast waves; usually only a small part of the flammable cloud is involved, so the blast effects are limited. In rare events, a high-power triggering event such as condensed-phase explosive or confined vapor cloud explosion can set off the detonation of the entire flammable cloud. The American Institute for Chemical Engineers (American Institute of Chemical Engineers 1994) estimates that direct initiation of detonation requires approximately one million Joules. The blast wave from the detonation of a large flammable cloud can have far-reaching effects; they can extend well beyond the area affected by the thermal radiation.

Damage is associated with both the shape and magnitude of the blast wave; both change as the wave travels outward from the reacting cloud. Peak overpressure and impulse are commonly used to characterize the blast wave. Wiekema reports a correlation between lung damage and the combination of overpressure and impulse (Wiekema 1984). Most studies of condensed phase explosions correlate injury with overpressure only. Clancey explained that the relationship between overpressure and impulse for condensed phase explosions is unique, so a single parameter is sufficient to describe the blast wave (Institution of Chemical Engineers (Great Britain). North Western Branch. 1982). Injuries and damage to structures from vapor cloud explosions depend on both overpressure and impulse; however, as with condensed phase explosions, most correlations use overpressure only. This simplification seems to be driven by the lack of data rather than any unique relationship between overpressure and impulse for vapor cloud explosions.

ALOHA uses only peak pressure to characterize the damaging effects associated with a blast wave. Harm can be due to direct effects or indirect effects of the pressure wave. Direct effects include damage to pressure-sensitive organs like ear and lung. Indirect effects can result from glass fragments from broken windows, collapse of buildings, or debris that is accelerated by the blast

wave. ALOHA includes three LOCs that quantify indirect and direct effects. Glass windows can shatter at 1 psi over ambient; at 3.5 psi there is a significant risk of eardrum rupture and injuries of serious nature from flying debris; at 8 psi there is significant risk of ear and lung damage and indirect effects from the collapse of unreinforced buildings (Baker 1983).

5.2 METHOD

ALOHA only models combustion reactions. ALOHA estimates the blast wave from unconfined vapor cloud explosions (fast deflagrations and detonations). Unconfined means that the cloud is not entirely or partially bounded by solid walls or ceilings. Confined vapor cloud explosions generally produce more damaging blast waves than unconfined or partially confined explosions.

The Baker-Strehlow-Tang (BST) model is the basis for the ALOHA overpressure calculation (Pierorazio et al. 2005); it uses non-dimensional, empirically derived blast curves to predict overpressure. The overpressure is based on the propagation speed of the flame front and the mass of fuel involved in the reaction. The basic principle of this method is that within the vapor cloud there are regions where physical structures can cause an acceleration of the flame front. These areas are characterized by the structure density using a parameter termed congestion. Flame speed is related to the chemical properties of the fuel, the level of congestion, and the nature of the ignition source.

Table 14. Baker-Strehlow-Tang flame speeds (Mach number). Mach 5.2 is used for deflagration to detonation transition (DDT).

	Low congestion	***medium congestion***	***High congestion***
High Reactivity	0.36	DDT	DDT
Medium Reactivity	0.11	0.44	0.5
low Reactivity	0.026	0.23	0.34

A reactivity term is used to characterize the chemical properties of the fuel. Reactivity ratings used by Zeeuwen and Wiekema (Zeeuwen and Wiekema 1978) classify reactivity based upon chemical laminar burning velocity in the BST model (Woodward 1998). Low-reactivity chemicals have velocities less than 45 cm/sec. High reactivity applies to those chemicals with burn velocities greater than 75 cm/sec and anything in between is labeled medium reactivity. Some chemicals in the ALOHA database were classified using this criteria; however, most of the flammable chemicals in ALOHA have not been classified. In these cases, ALOHA uses medium reactivity, since few chemicals have a laminar burning speeds exceeding 75 cm/sec.

A congestion parameter is used to quantify the way small structures within the vapor cloud affect the flame speed. Congestion refers to the density of obstacles that generate turbulence. Obstacles of this nature are generally small, like a shrub, and do not impede the flame front. Larger objects, like a building, can impede the flame front, so they should not be considered obstacles for the

purposes of congestion. Greater turbulence allows the flame front to accelerate, thereby generating a more powerful blast wave. The experiments that form the basis for the BST model found the flame speed could be related to area blockage ratio (cross sectional area of the structures divided by area of the cloud) and pitch (distance between rows of structures). The experiments used small structures arranged in regular patterns. Three levels of congestion could be distinguished: low congestion with an area blockage ratios less than 10%; medium congestion with area blockage ratio between 10% and 40%; and high congestion with higher blockage ratios. Extrapolating the laboratory parameters to what is found in an accidental explosion is highly imprecise so ALOHA greatly simplifies the use of congestion. Guidance in ALOHA requires the user to determine whether significant congestion is present. A congested zone is defined as one with so many closely spaced obstacles that it is difficult or impossible to walk through it; for example, pipe racks in industrial facilities and some forested areas where the trees and branches are closely spaced may be characterized as congested zones. To err on the side of caution, congestion defined this way is correlated with the high-congestion flame speed in the BST model.

The source of ignition also affects the flame speed. In ALOHA, the user inputs the ignition source. If the source is designated as a detonation, the model assumes that the triggering event is of sufficient power to cause the entire reactive cloud to detonate.

ALOHA's method for finding the normalized overpressure as a function of distance from the center of the explosive cloud is based on a set of empirically determined graphs (Pierorazio et al. 2005). BST reported normalized overpressure versus normalized distance from the center of the congested region with a different graph for different flame speeds. To implement these in ALOHA, the graphical data reported by BST were fit to functions of the form

$$\frac{\Delta P}{P_{atm}} = D \; if \; x < x_0,$$

$$else \; \frac{\Delta P}{P_{atm}} = A \cdot B^{1/x} x^C,$$

where ΔP is the maximum overpressure and A, B, C, D, and x_0 are constants. Table 15 gives values of these constants for various flame Mach numbers.

Table 15. Curve fit constants for various Mach numbers for use in the BST method.

	Mach 0.2	***Mach 0.35***	***Mach 0.7***	***Mach 5.2***
A	0.0335	0.1041	0.3764	0.2932
B	0.8359	0.8642	0.7439	1.399
C	-1.1192	-1.0568	-1.2728	-1.1591
D	0.065	0.22	0.65	20
x_0	0.35	0.32	0.3	0.16

The normalized distance, x is defined as

$$x = r\left(\frac{P_{atm}}{E}\right)^{1/3},$$

where
P_{atm} is the atmospheric pressure and
r is the distance from the center of the exploding cloud.

The energy contributing to the blast wave is

$$E = ref \cdot H_c \cdot Mass \ ,$$

where
ref is a ground reflection factor,
H_c is the heat of combustion of the fuel, and
$Mass$ is the mass of fuel involved in the explosion.

The ground reflection factor is set to 2 in ALOHA, consistent with the treatment by BST. It accounts for the reflection of the blast wave off the ground. ALOHA's treatment is based on a simplified conceptual model of the explosive cloud. The cloud is treated as a hemisphere at ground level with a uniform concentration. Elevated clouds would have a smaller reflection factor.

The most significant difference between the method in ALOHA and the Baker-Strehlow-Tang model is the method for determining the mass of fuel in the explosion. In the BST method, areas of congestion within a flammable cloud define the mass of fuel contributing to an explosion. The flame front propagates from the point of ignition, accelerates within regions of congestion, and decelerates outside the region of congestion. Only the mass of the fuel within a congested area contributes to the explosion. A flammable cloud emanating from a single release may give rise to as many explosions as there are distinct congested areas. The flame speeds are defined by the levels of congestion within those regions. Outside the congested areas the flame speed is assumed to be so slow that no significant overpressure is generated.

ALOHA uses a different approach for determining the mass of fuel involved in the explosion based on the recommendations of the American Institute for Chemical Engineers (American Institute of Chemical Engineers 1994). AIChE suggests that the BST blast curves can be coupled with an air dispersion model for determining the mass of the explosive cloud, using all the fuel within flammable limits times an efficiency factor. An efficiency factor of 5% to 20% is recommended; ALOHA uses 20%. ALOHA deviates slightly from the AIChE recommendation by using the fuel within a concentration range between the upper explosive limit and 90% of the lower explosive limit. This minor variation was introduced in ALOHA to create another conservative bias in the hazard zone calculation; it was not based on standard practices, theory, or measurement. Gas concentrations above the upper limit are presumed to be too rich, and those below the lower limit too lean, to participate in the explosion. The explosion of the flammable cloud is approximated as a single uniform event; the flame speed is based on the average level of congestion within the cloud. If the explosion is triggered by a high-power source, termed a hard ignition in ALOHA, or the

average level of congestion indicates a transition to detonation, 100% of the mass of the flammable cloud is used and Mach 5.2 is used for the flame speed.

The center of the explosive cloud is equated with the center of mass of flammable cloud in ALOHA. For non-steady-state releases the location of the center and mass of the flammable cloud changes with time. Users may choose the time of ignition; ALOHA then finds the flammable mass and center of the cloud, and generates overpressures as a function of distance. ALOHA can also compute all possible explosions from a single release and show the composite overpressure threat zone if the ignition time is not specified.

6 THERMAL RADIATION AND FLAMMABLE AREA MODELS

6.1 BACKGROUND

ALOHA models flame hazards associated with some common scenarios involving the combustion of liquids and gases. Fire scenarios involving chemicals with flashpoints exceeding 300°F cannot be modeled using ALOHA. Combustion scenarios are divided into two types in ALOHA: those that involve a fuel mixed with air to form a cloud with concentrations within the flammability range, and those involving an overly-rich core of fuel that burns at its outer edges (this includes pool fires where the rich core is the pool itself). ALOHA uses different methods for estimating the threat zones for these two types of scenarios.

Fires that burn on the surface of a rich core can burn for a long time. The hazard from thermal (infrared) radiation can extend well beyond the boundaries of the fire itself. Three models in ALOHA deal with these types of fires: Fireballs occur when a tank containing a flammable liquid explodes due to overpressurization and immediately ignites, commonly referred to as a BLEVE (the fire occurs at the surface of the fireball); Jet Fires occur when a flammable gas escapes from a pipe or tank (the fire occurs at the exit and burns at the edges of the rich core); and Pool Fires occur when a flammable liquid in a pool ignites and burns directly over the pool. There are two common empirical modeling approaches for these types of fires: point source models in which some fraction of the combustion energy is converted to thermal radiation and radiates from the center of the fire, and solid flame models in which the size and shape of the flame surface is found and radiation emitted from its surface are computed.

ALOHA employs solid flame models to compute thermal radiation hazards from fireballs, jet fires, and pool fires. In these three scenarios, the flux of thermal radiation emitted from the surface of the flame is computed, and the radiation impinging upon a distant target is found using

$$q = E \cdot F \cdot \tau ,$$

where
q is the thermal radiation flux incident on a vertical surface (W m^{-2}),
E is the thermal radiation energy flux at the surface of the fireball (W m^{-2}),
F is the geometric view factor, and
τ is the transmissivity of the atmosphere to thermal radiation.

Fuels that have been mixed with air before ignition burn quickly; the duration of the fire and the duration of the generated thermal radiation is generally quite short. Since the effects of thermal radiation scale with duration, the damaging effects usually do not extend very far beyond the boundaries of the flame itself. ALOHA address the hazard associated with fires that occur when a vapor cloud disperses downwind and forms a flammable mixture with air, ignites, and burns through the cloud by modeling the flammable area. ALOHA does not explicitly model the thermal radiation associated with flash fires.

6.2 LEVELS OF CONCERN FOR THERMAL RADIATION

The effects of thermal radiation are a function of the energy flux and the duration of exposure. For fires with expected durations exceeding about 30 seconds, the LOC is based upon the thermal radiation generated by the flame. Eisenberg analyzed data from nuclear weapons tests to determine the relationship between the intensity of thermal radiation and the probability that an exposed individual would be injured or killed (Eisenberg, Lynch, and Breeding 1975). He reported that the probability of a fatality is generally proportional to the duration of exposure (t_d) times the incident radiation flux (I) raised to the 4/3 power. For non-lethal effects, a power law of 1.15 fits the data better. The threshold for first degree burns was found when the exposure (in the form $I^{1.15}$ t_d) is 550,000 $(W/m^2)^{1.15}$ sec. Mudan reviewed Eisenberg's work as well as other studies that dealt with radiation sources that are less intense, but have longer duration (National Fire Protection Association 1995). The exposure laws described by Eisenberg obviously fail for very low, long-lived radiation sources; Mudan reports that an incident flux of 1.7 kW/m^2 will not even cause pain, regardless of exposure time. The apparent breakdown of the exposure law reported by Eisenberg is also reflected in the Safety Standards for Liquid Natural Gas Facilities in *Title 49 of the Code of Federal Regulations*. In calculating the radiation effects of pool fires, long-lived events, the Title 49 states that the radiation flux in an area of public assembly should be less than $5kW/m^2$, regardless of exposure time (United States Office of the Federal Register).

Burning pools, jets, and fireballs associated with a BLEVE can burn with sufficient longevity to create a persistent thermal radiation source that can cause harm far from the flame front itself. The impact on people depends on the both the duration of exposure and the intensity of the radiation. ALOHA computes the energy flux associated with the radiation as a function of distance and the duration of the fire and reports them separately. Even though dose values are associated with damage, energy flux values are used as LOCs in ALOHA since exposure time is a function of both the duration of the fire and the movement of individuals seeking some protection. ALOHA's LOCs are consistent with the recommendations of Mudan and Croce (National Fire Protection Association 1995): $10kW/m^2$ is a fatality threshold; $5kW/m^2$ can cause second degree burns on unprotected skin; and $2kW/m^2$ can cause pain. ALOHA refers to exposure durations of 60 seconds or less for these effects. The duration of the fire is included in the text summary screen of the ALOHA output allowing the user to adjust the flux levels to conform to the fire duration time.

6.3 BLEVE-FIREBALL

The BLEVE-Fireball model in ALOHA is a solid flame model based on studies of fireballs resulting from BLEVEs (boiling liquid expanding vapor explosions) involving flammable gases liquefied under pressure and stored at ambient temperatures, such as LPG (American Institute of Chemical Engineers 1994). In a common course of events, a fire impinges upon the tank, thermally stressing the tank and causing the internal pressure to rise. Pressure relief valves fail to adequately relieve the pressure and the tank explodes from the combination of heat and pressure. The contents are almost instantaneously released and quickly flash boil as they experience a drop in pressure. Much of the fuel, both liquid droplets and gas, is thrown into the air and ignites. The bulk of the burning mass is too rich to burn, but the fire burns at the surface where sufficient air can mix with the fuel. The resulting fireball burns for tens of seconds and often lifts into the air.

For a BLEVE scenario ALOHA assumes a near-instantaneous rupture and defaults to an assumption that the entire contents of a tank contribute to the fireball. However, in cases where the initial tank pressure is relatively low the user has an option of specifying the fraction of the contents that become part of the fireball. Based on the mass of fireball, the maximum diameter of the fireball is computed, approximating the fireball as a spherical object with its surface just touching the ground. (The fireball's diameter is a function of time; the maximum diameter is used in ALOHA to insure that hazard zones are not underestimated.) The flux of thermal radiation emitted from the burning surface is computed, and the radiation impinging upon a distant target is found. When the user specifies that less than 100% of the contents of the tank are in the fireball ALOHA assumes the remaining fuel forms a pool fire, and the pool fire model is used to find an alternate threat zone for thermal radiation. A limit of 5000 metric tons is employed as the maximum amount of chemical that can be modeled. This limit is of the order of the largest historical single BLEVE incident.

Though the probability of explosive rupture and fireball production is much lower for non-pressurized tanks, ALOHA extends the BLEVE-Fireball model to gases liquefied by refrigeration and volatile liquids with flash points below 300°F. Explosions of tanks containing pressurized gases can also generate fireballs of comparable size and duration (Zalosh and Weyandt 2005). However, ALOHA does not allow users to model the thermal radiation from fireballs associated with pressurized gases.

6.3.1 EMISSIVITY

AIChE states that 350 kW/m^2 is a reasonable emissive energy flux for large fireballs involving hydrocarbon fuels (American Institute of Chemical Engineers 1994). ALOHA applies this to a broader range of chemicals and sizes, but adjusts this value by multiplying by the ratio of the heat of combustion of the chemical divided by the heat of combustion of propane, and described as

$$E = 350,000\left(\frac{\Delta h_c}{\Delta h_{c,propane}}\right),$$

where

Δh_c is the heat of combustion of the chemical (J kg^{-1}), and

$\Delta h_{c,propane}$ is the heat of combustion of propane (J kg^{-1}).

6.3.2 VIEW FACTOR

The geometric view factor is a function of the size of the fireball and distance between a receptor and the fireball. The size depends upon the amount of the fuel contributing to the fireball. The user may choose to let ALOHA use the entire contents of the tank as the mass of the fireball, or have ALOHA calculate the fraction of the tank contents that contribute to the fireball based on the pressure or temperature of the tank at the time of rupture. If tank pressure is specified, the temperature at the time of rupture, T , is found using the Clausius-Clayperon equation, based on the assumption that two phases are present at equilibrium in the vessel, and described as

$$T = \left[\left(\frac{1}{T_B} \right) - \left(\frac{R_c}{\Delta H_V} \right) \ln \left(\frac{P}{P^0} \right) \right]^{-1} ,$$

where
T_B is the normal boiling point,
R_c is the gas constant (8.3144 J K^{-1} $mole^{-1}$),
ΔH_V is the heat of vaporization (J $mole^{-1}$),
P^0 standard pressure (101,000 Pa), and
P is the rupture pressure.

From the temperature, the fraction of liquid that flashes upon rupture is calculated. For an isenthalpic process the fraction that flashes is given by

$$f = \frac{C_p \left(T - T_b \right)}{\Delta H_v} ,$$

where
T is the chemical temperature at tank failure (K),
T_b is the ambient boiling point (K),
C_p is the specific heat capacity at constant pressure (J $mole^{-1}$ K^{-1}), and
ΔH_v is the heat of vaporization (J/mole).

This somewhat overestimates the fraction that flashes in an adiabatic (isentropic) process, but provides a reasonable approximation.

An empirical correlation indicates that mass of chemical participating in the fireball is about three times the mass of fuel that flash boils upon rupture, limited to the total mass of the contents of the tank (Hasegawa and Sato 1977).

ALOHA adopted the recommendation of Roberts for computing the diameter of a fireball (Roberts 1982):

$$D_{\max} \left(meters \right) = 5.8 mass^{1/3} \left(kg \right).$$

The geometric view factor for a vertical surface, F, was given by AIChE (American Institute of Chemical Engineers 1994) as

$$F = \frac{x\left(D_{\max}/2\right)^2}{\left(x^2 + \left(D_{\max}/2\right)^2\right)^{3/2}} \quad for \quad x > \left(D_{\max}/2\right),$$

where x is the distance between a receptor and a point at ground level directly below the center of the fireball.

6.3.3 TRANSMISSIVITY

The transmissivity of the atmosphere to thermal radiation, τ, depends upon the distance between the emitting and receiving surfaces, x. It is sensitive to fog, rain, smoke, carbon dioxide, and water vapor in the atmosphere. ALOHA only accounts for water vapor. By neglecting the other factors, ALOHA overestimates the transmitted radiation in cases where the other attenuating phenomena occur. Transmissivity of the atmosphere to thermal radiation, τ, is well studied. ALOHA uses the formula reported by Cook et al. (Cook, Bahrami, and Whitehouse 1990),

$$\tau = 1.389 - 0.135 \log_{10}(P_w x).$$

ALOHA uses the formula reported by Thibodeaux for the partial pressure of water in the atmosphere (Thibodeaux 1979),

$$P_w = 99.89 \frac{R_H}{100} \exp\left(21.66 - \frac{5431.3}{T_a}\right),$$

where
T_a is the ambient air temperature and
R_H is the relative humidity.

6.3.4 DURATION

The duration of the fire, t_{burn}, is not used in the computation of the hazard zone, but is displayed.

ALOHA uses the formula recommended by the Dutch Committee for Prevention of Disasters (Duiser 1992), which was based upon averages obtained from reported literature values,

$$t_{burn}(\text{sec}) = 0.852 mass^{0.26}(kg).$$

6.4 JET FIRES

The jet fire analysis in ALOHA is designed to address the thermal radiation hazards associated with gases and aerosols released from pressurized tanks and pipes which ignite before the vapors disperse downwind. Jet fires differ from flash fires in that they completely burn immediately upon release at the surface of a fuel-rich core. Jet fires differ from fireballs in that jet fires are associated with sustained releases, while fireballs are associated with an explosive tank rupture due to overpressurization.

The Jet Fire model in ALOHA can be applied to an upward vertical jet release: a pipe oriented vertically or a hole at the top of a tank. The method in ALOHA is based on an empirical solid flame model developed by Shell Research (Chamberlain 1987). Fuel released from the pipe or tank expands, mixes with air, and burns on its surface emitting intense thermal radiation that propagates outward. The thermal energy incident upon a distant target is a product of the emissivity of the flame surface, the geometric view factor, and the transmissivity of the atmosphere to thermal radiation.

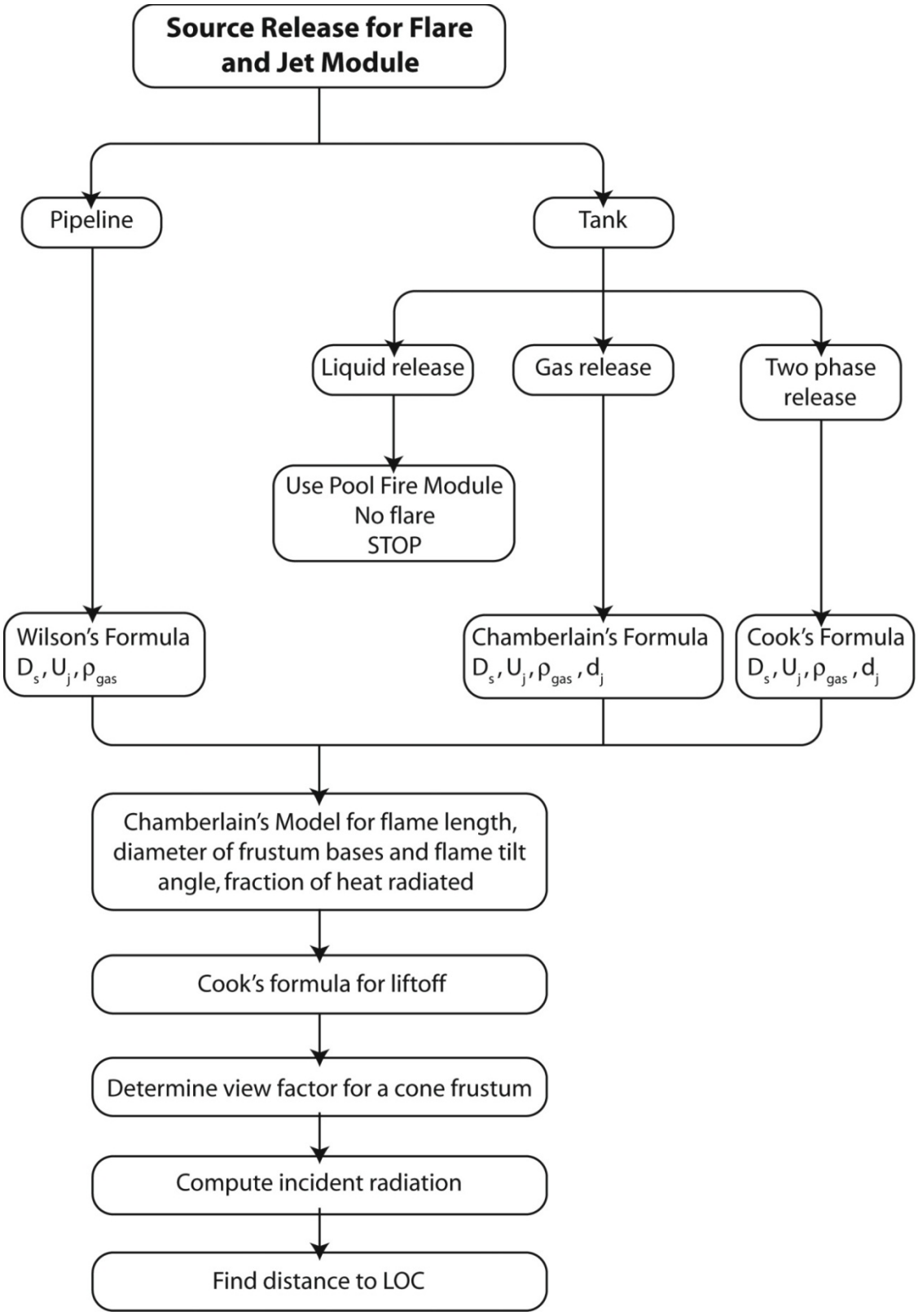

Figure 3. Source release for jet fire flowchart.

6.4.1 EMISSIVITY

From Cook et al (Cook, Bahrami, and Whitehouse 1990), the emissive power of the flame, *E*, is calculated as

$$E = \frac{f_{rad} Q \Delta h_c}{A},$$

where

Q is the mass discharge rate (kg s^{-1}),

Δh_c is the heat of combustion (J kg^{-1}), and

A is the surface area of the flame (m^2).

From Chamberlain (Chamberlain 1987), the fraction of heat radiated from the flame surface is

$$f_{rad} = 0.21 C_{MW} \exp(-0.00323 u_j) + 0.11.$$

Where C_{MW} is a correction factor introduced by Cook et al (Cook, Bahrami, and Whitehouse 1990) equal to unity if the molecular weight is less than 21 g $mole^{-1}$, the square root of the molecular weight divided by 21 if the molecular weight is between 21 g $mole^{-1}$ and 60 g $mole^{-1}$, and equal to 1.69 if the molecular weight is greater than 60 g $mole^{-1}$.

The gas velocity in the expanding jet is

$$u_j = M_j \sqrt{\frac{\gamma_g R_c T_j}{W_{gk}}}$$

and

$$T_j = \frac{2T_s}{2 + (\gamma_g - 1) M_j^2},$$

where T_s is temperature inside vessel or at exit of pipe.

For unchoked flow, the Mach number of the expanded jet, M_j, is calculated by

$$M_j = \left[\frac{\left(1 + 2(\gamma_g - 1) F^2\right)^{\frac{1}{2}} - 1}{(\gamma_g - 1)} \right]^{\frac{1}{2}} \text{ and}$$

$$F = 3.6233 \cdot 10^{-5} \frac{Q}{d_o^2} \sqrt{\frac{T_s}{\gamma_g W_{gk}}},$$

where
d_o is the diameter of the orifice,
Q is the mass release rate,
γ_g is the ratio of specific heats,
W_{gk} is the molecular weight (kg mole^{-1}), and
R_c is the gas constant (8.3144 J K^{-1} mole^{-1}).

6.4.2 VIEW FACTOR

The flame surface is approximated as a frustum of a cone tilted by the wind.

The effective source diameter is the throat diameter of an imagined nozzle from which air at normal ambient density issues at the gas mass flow rate and exit velocity. The effective source diameter for a gas is

$$D_s = d_o \sqrt{\frac{\rho_j}{\rho_{air}}},$$

where
d_o is the diameter of the exit orifice, and
ρ_j is the density of the gas.

For choked flow the Mach number is

$$M_j = \sqrt{\frac{\left(\gamma_g + 1\right)\left(\frac{P_c}{P_o}\right)^{\frac{\left(\gamma_g - 1\right)}{\gamma_g}} - 2}{\left(\gamma_g + 1\right)}},$$

where
P_o is atmospheric pressure,
P_c is static pressure at the exit orifice, and

$$P_c = 3.6713 \frac{Q}{d_o^2} \sqrt{\frac{T_c}{\gamma_g W_{gk}}},$$

$$T_c = \frac{2T_s}{1+\gamma_g}$$

where T_s is the temperature inside the vessel or at the exit of the pipe.

The jet expands to atmospheric pressure at a plane downstream of the exit hole with the plane acting as a virtual source of diameter, d_j. Then,

$$D_s = d_j \sqrt{\frac{\rho_j}{\rho_{air}}} \text{ and}$$

$$d_j = \sqrt{\frac{4Q}{\pi u_j \rho_j}} = \sqrt{\frac{4Q}{\pi P_o M_j}} \sqrt{\frac{R_c T_j}{\gamma_g W_{gk}}} = \sqrt{3.6233 \cdot 10^{-5} \frac{Q}{M_j}} \sqrt{\frac{T_j}{\gamma_g W_{gk}}},$$

where u_j is the velocity of the gas in the expanded jet.

These formulas were modified slightly for the pipeline jet fire and two-phase release scenarios. ALOHA assumes that the gas expands adiabatically in the last 200 pipe diameters in the pipeline release. It exits at atmospheric pressure and therefore the effective source diameter, D_s for the choked option reduces to that for the unchocked option given earlier. For two-phase release, ALOHA uses a modification of the formula in Cook et al. (Cook, Bahrami, and Whitehouse 1990),

$$D_s = d_j \left(\frac{\rho_j \rho_v}{\rho_{air}^2} \right)^{1/4},$$

where ρ_v is the pure vapor density.

The modification of the Cook formula was necessary to insure that it would reduce to the proper algorithm when the two-phase case reduced to the pure gas scenario.

For a tilted jet, Kalghatgi (Kalghatgi 1983) showed in laboratory experiments that the flame length reduces as the jet is tilted into the wind. Chamberlain uses Kalghatgi's empirical fit equation to determine the flame length, L_B (Kalghatgi 1983) as

$$L_B = 105.4 D_s \left[1 - 6.07 \cdot 10^{-3} \left(\theta_j - 90 \right) \right].$$

The flame length in still air is

$$L_{Bo} = \frac{L_B}{\left[0.51 \exp\left(-0.4 v \right) + 0.49 \right] \left[1 - 6.07 \cdot 10^{-3} \left(\theta_j - 90 \right) \right]}.$$

The angle, α, between the orifice axis and the flame depends on the velocity ratio, is

$$R = \frac{V}{u_j},$$

where V is the wind speed.

If $R \le 0.05$, then

$$\alpha = \frac{8000R + \xi\left(L_{Bo}\right)\left(\theta_j - 90\right)\left(1 - \exp\left(-25.6R\right)\right)}{\xi\left(L_{Bo}\right)},$$

and if $R > 0.05$, then

$$\alpha = \frac{\left[1726\sqrt{R - 0.026} + 134\xi\left(L_{Bo}\right)\left(\theta_j - 90\right)\left(1 - \exp\left(-25.6R\right)\right)\right]}{\xi\left(L_{Bo}\right)} \text{ and}$$

$$\xi\left(L_{Bo}\right) = L_{Bo}\left[\frac{g}{D_s^2 u_j^2}\right]^{\frac{1}{3}}.$$

The flame-lift off, b, is the distance along the axis of the cone, and is calculated as

$$b = 0.015L_B \text{ for aerosols, and } b = L_B \frac{\sin K\alpha}{\sin \alpha} \text{ for gases.}$$

K has been correlated with experimental data with a best fit of

$$K = 0.185e^{-20R} + 0.015.$$

The frustum length is given by the geometrical relationship between R_L, L_B, α and b, as

$$R_L = \sqrt{\left(L_B^2 + b^2 \sin^2 \alpha\right)} - b\cos\alpha\,.$$

There appears to be a difference in the formula for the width of the frustum base as it appears in Chamberlain's paper when compared to Lees (Lees 2001) presentation of Chamberlain's formula. Based on sample calculations, we determined to use the Chamberlain's version (Chamberlain p. 303) with the width of the frustum base., W_1, as

$$W_1 = D_s\left[13.5\exp\left(-6R\right) + 1.5\right]\left\{1 - \left[1 - \frac{1}{15}\left(\frac{\rho_a}{\rho_j}\right)^{\frac{1}{2}}\right]\exp\left(-70\xi\left(D_s\right)^{CR}\right)\right\},$$

where

$$C = 1000\exp\left(-100R\right) + 0.8$$

and the Richardson number, $\xi(D_s)$, based on D_s is

$$\xi(D_s) = \left(\frac{g}{D_s^2 u_j^2} \right)^{\frac{1}{3}} D_s .$$

The Chamberlain formula for the width at frustum tip, W_2, is

$$W_2 = L_B \left(0.18\exp\left(-1.5R\right) + 0.31\right)\left(1 - 0.47\exp\left(-25R\right)\right).$$

The surface area of the flame, *A*, is calculated as

$$A = \frac{\pi}{4}\left(W_1^2 + W_2^2\right) + \frac{\pi}{2}\left(W_1 + W_2\right)\left[R_L^2 + \left(\frac{W_2 - W_1}{2} \right)^2 \right]^{\frac{1}{2}} .$$

The view factor F is defined by Sparrow and Cess (Sparrow and Cess 1978) as

$$dF_{A_j - dA_i} = \frac{dA_i}{A_j} \int_{A_j} \frac{\cos\beta_i \cos\beta_j dA_j}{\pi r^2},$$

where

A_j is the area of the radiating surface;

dA_i is the receiving element;

β_i is the angle between the normal to the receiving element and the line between the element and the radiating surface;

β_j is the angle between the normal to the radiating surface at a point and the line between that point and the receiving element; and

r is the distance between the point on the radiating surface and the receiving element.

For a radiating surface of area A_i and a receiving element of area dA_j, we can let

q' = incident radiation intensity per unit area, and

E' = emissive power per unit area,

so that

$$q' = \frac{q}{dA_i} = \frac{E \cdot F \cdot \tau}{dA_i} = \frac{E' \cdot A_j \cdot F \cdot \tau}{dA_i} = E' \cdot \left(\frac{A_j}{dA_i} \cdot F \right) \cdot \tau .$$

Thus, it is actually $\int_{A_j} \frac{\cos\beta_i \cos\beta_j dA_j}{\pi r^2}$ that we need to calculate.

We calculate this integral numerically by dividing the flame surface into 1800 "tiles" (40 radial divisions x 25 axial divisions of the conical surface, plus 400 tiles for each circular "cap"). The value of the integrand is calculated at the center of each tile, and those values are added to produce an estimate of the integral. This process is carried out for three orthogonal orientations of the receiving surface, producing view factors f_1, f_2, and f_3. The maximum view factor (over all orientations of the receiving surface) is then calculated as

$$f = \sqrt{f_1^{\,2} + f_2^{\,2} + f_3^{\,2}}\,.$$

(For a true view factor, the integral omits portions of the radiating surface where $\cos\beta_j$ <0. But since f_1, f_2, and f_3 are used to calculate the maximum view factor, portions where $\cos\beta_j$ <0 are not excluded.)

6.5 POOL FIRES

There are 3 release scenarios that can be coupled with the Pool Fire model: The user may choose to model a pool of constant area that is not associated with a tank release; the Pool Fire model can also be coupled with a model that estimates the pool formation dynamics when a tank of chemical is leaking; and the Pool Fire model is automatically applied to any fuel that pools during a BLEVE scenario. In all cases, the pool is assumed to be circular, uniformly thick, and on a level surface. The pool temperature is approximated as a constant and set to either the initial pool temperature or the initial tank temperature. A 200-meter diameter limit applies in all cases.

A solid flame model is used to calculate the thermal radiation from pool fires. The size of the pool can be set by the user, or ALOHA will calculate the dynamic area and volume from the release of a liquid from a tank. The flames rising from the pool form a tilted cylinder; the surface of the cylinder radiates thermal radiation. Burn rate, flame height, angle of tilt, and emission of radiation from the surface are based on empirical correlations.

The thermal energy incident upon distant target is the product of the thermal radiation energy flux at the surface of the flame, the geometric view factor, and the transmissivity of the atmosphere to thermal radiation.

6.5.1 EMISSIVITY

The average emissive power per unit area, *E*, of the cylinder surface is estimated using the approach of Moorhouse and Pritchard (Moorhouse and Pritchard 1982),

$$E = \frac{f_{rad}\Delta h_c \dot{m}}{\left(1+4\frac{h}{d}\right)},$$

where
h is the flame length (m),
d is the diameter of the pool (m),
Δh_c is the heat of combustion (J kg^{-1}),
$\dot{m}$ is the mass burn rate per unit area (kg m^{-2} s^{-1}), and
f_{rad} is the fraction of energy released as thermal radiation.

ALOHA approximates the fraction of energy radiated, f_{rad}, as a constant 30% as suggested by Roberts (Roberts 1982).

The mass burn rate per unit area, $\dot{m}$, is calculated from ratios of the heats of combustion and vaporization. Mudan states that the following correlation for the mass burning rate fits a wide range of fuels including liquefied gases (Mudan 1984):

$$\dot{m} = 0.001 \cdot \frac{\Delta h_c}{\Delta h_v}.$$

ALOHA uses a modified version of this with a correction for temperature, given as

$$\dot{m} = 0.001 \cdot \frac{\Delta h_c}{\Delta h_v + c_p \left(T_b - T \right)},$$

where
c_p is the specific heat capacity (J kg^{-1} K^{-1}),
T_b is the ambient boiling temperature (K),
Δh_v is the heat of vaporization (J kg^{-1}), and
T is the pool temperature (K).

6.5.2 VIEW FACTOR

The flame of the pool fire is assumed to be an optically dense tilted cylinder which intersects a plane parallel to the ground in a circle. The flame length, *h*, is estimated by a modification of the Thomas formula for flame length (Thomas 1963). Let u^* be a non-dimensional wind velocity defined as

$$u^* = u \cdot \left(\frac{\rho_a}{g \cdot \dot{m} \cdot d} \right)^{1/3}.$$

The flame length is given by

$$h = d \cdot 55 \cdot \left(\frac{\dot{m}}{\rho_a \cdot \sqrt{g \cdot d}} \right)^{0.67} \cdot \left(u^* \right)^{-0.21},$$

where
ρ_a is the density of ambient air (kg m^{-3}).

The angle of tilt is based on formulas from the American Gas Association (American Gas Association 1973), and is given by

$$\theta = 0 \quad if\ u^* \le 1,$$
$$\theta = \cos^{-1}\frac{1}{\sqrt{u^*}} \quad if\ u^* > 1.$$

The view factor F is defined by Sparrow and Cess (Sparrow and Cess 1978) as

$$dF_{A_j - dA_i} = \frac{dA_i}{A_j}\int_{A_j}\frac{\cos\beta_i \cos\beta_j dA_j}{\pi r^2},$$

where
A_j is the area of the radiating surface;
dA_i is the receiving element;
β_i is the angle between the normal to the receiving element and the line between the element and the radiating surface;
β_j is the angle between the normal to the radiating surface at a point and the line between that point and the receiving element; and
r is the distance between the point on the radiating surface and the receiving element.

For a radiating surface of area A_i and a receiving element of area dA_j, we can let
q' = incident radiation intensity per unit area, and
E' = emissive power per unit area,

so,

$$q' = \frac{q}{dA_i} = \frac{E \cdot F \cdot \tau}{dA_i} = \frac{E' \cdot A_j \cdot F \cdot \tau}{dA_i} = E' \cdot \left(\frac{A_j}{dA_i} \cdot F\right) \cdot \tau .$$

Thus, it is actually $\int_{A_j}\frac{\cos\beta_i \cos\beta_j dA_j}{\pi r^2}$ that we need to calculate.

We calculate this integral numerically by dividing the flame surface into 1000 "tiles" (40 radial divisions x 25 axial divisions). The value of the integrand is calculated at the center of each tile[5], and those values are added to produce an estimate of the integral. This process is carried out for

[5] For tiles at the base of the flame surface, the point used is on the ground, not the tile center. This permits greater accuracy when calculating view factors for observers near the surface.

three orthogonal orientations of the receiving surface, producing view factors f_1, f_2, and f_3. The maximum view factor (over all orientations of the receiving surface) is then calculated as

$f = \sqrt{f_1^{\,2} + f_2^{\,2} + f_3^{\,2}}$. (For a true view factor, the integral omits portions of the radiating surface where $\cos\beta_j$ <0. But since f_1, f_2, and f_3 are used to calculate the maximum view factor, portions where $\cos\beta_j$ <0 are not excluded.)

6.5.3 POOL DYNAMICS

The maximum diameter of the pool is used in all the above calculations. In cases where the pool size is dynamic because chemical is released during a BLEVE or from a leaking tank, ALOHA uses the same tank release and pool growth methods as those used for non-thermal hazards.

For tank release rates, ALOHA uses Bernoulli's equation to compute $Q_T(t)$ (kg s^{-1}), the mass flow of liquid from the hole,

$$Q_T(t) = C_{dis} A_f \sqrt{2(P_h - P_a)\rho_l},$$

where
C_{dis} is the discharge coefficient (0.61),
A_f is the flow area (m^2),
P_h is the pressure of the liquid in the tank at the height of the hole (Pa),
P_a is the ambient atmospheric pressure (Pa), and
ρ_l is the density of the liquid in the tank (kg m^{-3}), which is assumed to be uniform throughout the tank.

ALOHA estimates the flow area, A_f (m^2), differently depending on whether or not the liquid surface intersects the hole. The flow area is

$$A_f(t) = \begin{cases} A_h & \text{surface above hole,} \\ A_h(h_l/\zeta_h) & \text{surface intersects hole,} \end{cases}$$

where
h_l is the height of the liquid above the bottom of the hole (m), and
ζ_h is either the hole height or diameter (m), depending on whether the hole is rectangular or circular.

When the hole is below the liquid surface, ALOHA estimates the pressure at the hole as the sum of the pressure within the gas void at the top of the tank and the pressure exerted by the column of liquid above the bottom of

$$P_h(t) = \begin{cases} e_{cs} + h_l \rho_l g & \text{surface above the hole,} \\ p_a + h_l \rho_l g & \text{surface intersects the hole,} \end{cases}$$

where e_{cs}, the saturated vapor pressure of the chemical (Pa), is assumed to be the pressure within the void space.

Because ALOHA assumes that the sequence of pressure drop, evaporation of liquid into the void space, and temperature change caused by evaporative cooling occurs rapidly during each new time step, it computes a new temperature and saturated vapor pressure for the vapor in the void space. As the liquid height above the hole bottom decreases, the pressure at the hole decreases until it eventually equals atmospheric pressure. According to the physical model represented by ALOHA's algorithms, tank outflow then stops until an air bubble is ingested back into the tank, equalizing tank and atmospheric pressure and allowing flow to continue as a series of gushes. To approximate the effect of this process mathematically, once ALOHA's computed pressure at the hole reaches 1.01 P_a, it is held constant at that value (Belore and Buist 1986).

If liquid spills into a puddle faster than the puddle burns, the puddle will grow deeper and will spread outward under the influence of gravity. The puddle is approximated with uniform depth and temperature. ALOHA estimates the change in puddle radius, r_p, as

$$\frac{dr_p}{dt} = \frac{1}{r_p}\sqrt{\frac{2gm_p}{\pi\rho_l}},$$

where m_p is the dynamic mass of the puddle, g is the acceleration of gravity, r_p is the puddle radius, and ρ_l is the density of the liquid in the puddle. ALOHA uses a constant factor of 2 to account for the fact that the inertia of the spreading liquid is only a fraction of the inertia of the whole liquid-pool mass moving with the acceleration at its leading edge (Briscoe and Shaw 1980). When the puddle depth drops below 0.5 cm, ALOHA stops spreading; the area is held constant until the liquid has completely burned away.

6.6 FLASH FIRES AND FLAMMABLE AREA

The Flammable Area analysis in ALOHA is designed to address the hazards associated with a fire or explosion of a cloud composed of a mixture of flammable chemical vapors and air in proportions that will support the propagation of a flame. The flammable area represents the region where an ignition source can lead to a flash fire or vapor cloud explosion, and the area where the fire can occur. While a vapor cloud explosion can generate a damaging shock waves outside the flammable area, the fire hazard associated with a flash fire usually does not.

Typically with flash fires of premixed clouds, the thermal radiation generated is highly transient. ALOHA does not explicitly model the thermal radiation associated with a flash fire, rather uses the approach of the US EPA (United States. Environmental Protection Agency. Chemical Emergency Preparedness and Prevention Office 1999) and assumes that the threat zone from a flash fire is closely related to the lower flammability or explosive limit threat zone (ground level concentration contour) for the cloud. Based upon recommendations of the project external review team the choice was made to use 60% of the lower flammability limit as the level of concern in defining this threat zone. This value reflects the fact that the concentration calculation in ALOHA involves some time averaging. Therefore, there is the possibility that a location with an average concentration below the LEL may have a fluctuating concentration that sometimes exceeds the LEL.

Modeling the thermal hazard associated with flash fires employs source strength models and air dispersion models that are part of the toxic air plume analysis in ALOHA. Any location where the gas concentration exceeds 60% of the LEL at any time following the release is included in the hazard zone.

7 BIBLIOGRAPHY

American Gas Association. 1973. *LNG Information Book*. Arlington, VA: National Technical Information Service.

American Institute of Chemical Engineers. *DIPPR 801* [Database]. American Institute of Chemical Engineers, July 2013. Available from http://www.aiche.org/dippr/.

American Institute of Chemical Engineers. 1994. *Guidelines for evaluating the characteristics of vapor cloud explosions, flash fires, and BLEVEs*. New York, NY: Center for Chemical Process Safety of the American Institute of Chemical Engineers.

American Institute of Chemical Engineers. Center for Chemical Process Safety. 1989. *Workbook of test cases for vapor cloud dispersion models*. New York, NY: Center for Chemical Process Safety of the American Intstitute of Chemical Engineers.

Baker, W. E. 1983. *Explosion hazards and evaluation*. Amsterdam; New York: Elsevier Scientific Pub. Co.

Barsan, Michael E., United States. Dept. of Health and Human Services., and National Institute for Occupational Safety and Health. 2010. *NIOSH pocket guide to chemical hazards*, *NIOSH Publication no. 2010-168c*. Atlanta, Ga.: Centers for Disease Control and Prevention.

Beals, Gordon Alden. 1971. *Guide to local diffusion of air pollutants*. Scott AFB, Ill.,: Air Weather Service (MAC), U.S. Air Force.

Bell, R.D. 1978. "Isopleth calculations for ruptures in sour gas pipelines." *Energy Processing Canada* no. 71 (4):36-39.

Belore, R, and I Buist. 1986. A computer model for predicting leak rates of chemicals from damaged storage and transportation tanks. edited by Environmental Emergencies Technology Division: Environment Canada.

Blevins, Robert D. 1984. *Applied fluid dynamics handbook*. New York, N.Y.: Van Nostrand Reinhold Co.

Blewitt, D. N. 1990. Personal Communication with ALOHA Development Team. Seattle.

Brand, J.C.D., and A. Rutherford. 1952. "The Vapour Pressure of the System Sulphuric Acid - Disulphuric Acid." *Journal of the Chemical Society* no. 10:3916-3922.

Briggs, G. A. 1991. Personal communication.

Briggs, Gary A. 1973. *Diffusion estimation for small emissions : preliminary draft*. Oak Ridge, TN: Atmospheric Turbulence and Diffusion Laboratory.

Brighton, P. W. M. 1985. "Evaporation from a Plane Liquid Surface into a Turbulent Boundary-Layer." *Journal of Fluid Mechanics* no. 159 (Oct):323-345.

Brighton, P. W. M. 1990. "Further Verification of a Theory for Mass and Heat-Transfer from Evaporating Pools." *Journal of Hazardous Materials* no. 23 (2):215-234.

Briscoe, F., and P. Shaw. 1980. "Spread and Evaporation of Liquid." *Progress in Energy and Combustion Science* no. 6 (2):127-140.

Britter, R. E. 1989. "Atmospheric Dispersion of Dense Gases." *Annual Review of Fluid Mechanics* no. 21:317-344.

Brutsaert, Wilfried. 1982. *Evaporation into the atmosphere: theory, history, and applications*, *Environmental fluid mechanics*. Dordrecht, Holland; Boston; Hingham, MA: Reidel; Sold and distributed in the U.S.A. and Canada by Kluwer Boston.

Businger, J. A. 1973. Turbulence transfer in the atmospheric surface layer. In *Workshop on Micrometeorology*, edited by D. A. Haugen. Boston: American Meteorological Society.

Chamberlain, G. A. 1987. "Developments in Design Methods for Predicting Thermal-Radiation from Flares." *Chemical Engineering Research & Design* no. 65 (4):299-309.
Chemwatch. 2006. 2006]. Available from http://www.chemwatch.net.
Cochran, William G., and Gertrude Mary Cox. 1957. *Experimental designs*. 2nd ed, *Wiley publications in applied statistics)*. New York: Wiley.
Colenbrander, G. W. 1980. A Mathematical Model for the Transient Behavior of Dense Vapor Clouds. In *3rd International Symposium on Loss Prevention and Safety Promotion in the Process Industries*. Basel, Switzerland.
Colenbrander, G. W., and J. S. Puttock. 1983. Dense Gas Dispersion Behavior: Experimental Observations and Model Developments. In *International Symposium on Loss Prevention and Safety Promotion in the Process Industries.* Harrogate, England.
Cook, J., Z. Bahrami, and R. J. Whitehouse. 1990. "A Comprehensive Program for Calculation of Flame Radiation-Levels." *Journal of Loss Prevention in the Process Industries* no. 3 (1):150-155.
Deacon, E.L. 1973. "Geostrophic drag coefficients." *Boundary Layer Meteorology* no. 5 (4):321-340.
Dodge, F., E. Bowels, and R. White. 1980. Release rates of hazardous chemicals from damaged cargo vessels. Paper read at National Conference on Control of Hazardous Materials Spills.
Duiser, J.A. 1992. "Chapter 6. Heat Radiation." In *Methods for the calculation of physical effects, Second edition*. Voorburg: Committee for the Prevention of Disasters.
Eisenberg, N., C.J. Lynch, and R.J. Breeding. 1975. Vulnerability model: a simulation system for assessing damage resulting from marine spills. National Technical Information Service.
Environmental Protection Service. 1984. *Sulfuric Acid and Oleum*, *Environmental and technical information for problem spills manuals*. Ottawa: Environment Canada EPS.
Fackrell, J. E., and A. G. Robins. 1982. "Concentration Fluctuations and Fluxes in Plumes from Point Sources in a Turbulent Boundary-Layer." *Journal of Fluid Mechanics* no. 117 (Apr):1-26.
Fauske, H. K. 1985. "Flashing flow or some practical guidelines for emergency releases." *Plant/Operations Progress* no. 4 (3).
Fauske, H. K., and M. Epstein. 1987. Source term considerations in connection with chemical accidents and vapor cloud modeling. In *International Conference on Vapor Cloud Modeling*. Cambridge.
Fisher, H. G., H. S. Forrest, S. S. Grossel, and American Institute of Chemical Engineers. The Design Institute for Emergency Relief Systems. 1992. *Emergency relief system design using DIERS technology: The Design Institute for Emergency Relief Systems (DIERS) project manual*. New York: Wiley Interscience: The Design Institute for Emergency Relief Systems of the American Institute of Chemical Engineers.
Frouin, R., D. W. Lingner, C. Gautier, K. S. Baker, and R. C. Smith. 1989. "A Simple Analytical Formula to Compute Clear Sky Total and Photosynthetically Available Solar Irradiance at the Ocean Surface." *Journal of Geophysical Research-Oceans* no. 94 (C7):9731-9742.
Grimsrud, D., M. Sherman, and R. Sonderegger. 1983. Calculating Infiltration: Implications for a Construction Quality Standard. edited by Lawrence Berkeley Laboratory. Berkeley: Lawrence Berkeley Laboratory.
Grolmes, M.A., and H.G. Fisher. 1994. Vapor-Liquid Onset/Disengagement Modeling for Emergency Relief Discharge Evaluation. edited by Robert Jones.
Hanna, Steven R., Gary A. Briggs, Rayford P. Hosker, United States. Dept. of Energy. Office of Energy Research., and United States. Dept. of Energy. Office of Health and Environmental Research. 1982. *Handbook on atmospheric diffusion: prepared for the Office of Health and Environmental Research, Office of Energy Research, U.S. Department of Energy*. [Oak Ridge, TN]: Technical Information Center, U.S. Dept. of Energy.

Hasegawa, K., and K. Sato. 1977. Study on the fireball following steam explosion of n-pentane. Paper read at Second International Symposium on Loss Prevention and Safety Promotion in the Process Industry, at Heidelburg.
Havens, J. 1990. NOAA Degadis Evaluation Report.
Havens, Jerry A., and Thomas O. Spicer. 1985. *Development of an Atmospheric Dispersion Model for Heavier-Than-Air Gas Mixtures. Volume 1*. Ft. Belvoir: Defense Technical Information Center.
Henry, R. E., and H. K. Fauske. 1971. "2-Phase Critical Flow of One-Component Mixtures in Nozzles, Orifices, and Short Tubes." *Journal of Heat Transfer* no. 93 (2):179-187.
Huff, J. E. 1985. "Multiphase flashing flow in pressure relief systems." *Plant/Operations Progress* no. 4 (3).
Institution of Chemical Engineers (Great Britain). North Western Branch., European Federation of Chemical Engineering. 1982. *The assessment of major Hazards*. 1st ed, *EFCE publication series ;*. Rugby, Warwickshire; Oxford, England; Elmsford, N.Y.: Institution of Chemical Engineers.
Kalghatgi, G. T. 1983. "The Visible Shape and Size of a Turbulent Hydrocarbon Jet Diffusion Flame in a Cross-Wind." *Combustion and Flame* no. 52 (1):91-106.
Karlins, WIlliam. 1994. Personal Communication with Robert Jones.
Kawamura, Peter, D. MacKay, Canada. Environmental Emergencies Technology Division., Canada. Environmental Protection Service., Canada. Environment Canada., and Canada. Technology Development and Technical Services Branch. 1985. *The evaporation of volatile liquids*. Ottawa: Environmental Emergencies Technology Division, Technical Services Branch, Environmental Protection Service, Environment Canada.
Kirk, Raymond E., Donald F. Othmer, David Eckroth, and Martin Grayson. 1978. *Encyclopedia of chemical technology*. 3rd ed. 31 vols. New York: Wiley.
Kirk, Raymond E., Donald F. Othmer, Jacqueline I. Kroschwitz, and Mary Howe-Grant. 1991. *Encyclopedia of chemical technology*. 4th ed. New York: Wiley.
Lees, Frank P. 2001. *Loss prevention in the process industries: hazard identification, assessment, and control*. 2nd ed. 3 vols. Boston: Butterworth-Heinemann.
Leung, J. C. 1994. Personal Communication with Robert Jones.
Lide, David R. 1993. *CRC handbook of chemistry and physics*. 74th ed. 1 vols. Boca Raton ; London: CRC Press.
Moorhouse, J., and M. Pritchard. 1982. "Thermal radiation hazards from large pool fires and fireballs." In *Industrial Chemical Engineering Symposium Series*.
Mudan, K. S. 1984. "Thermal-Radiation Hazards from Hydrocarbon Pool Fires." *Progress in Energy and Combustion Science* no. 10 (1):59-80.
National Fire Protection Association. 1995. *SFPE handbook of fire protection engineering*. 2nd ed. Quincy, Mass.: National Fire Protection Association.
Palazzi, E., M. Defaveri, G. Fumarola, and G. Ferraiolo. 1982. "Diffusion from a Steady Source of Short Duration." *Atmospheric Environment* no. 16 (12):2785-2790.
Pasquill, F. 1961. "The Estimation of the Dispersion of Windborne Material." *Meteorology Magazine* no. 90:33 - 49.
Perry, Robert H., Don W. Green, and James O. Maloney. 1984. *Perry's Chemical engineers' handbook*. 6th ed, *McGraw-Hill chemical engineering series.* New York: McGraw-Hill.
Pierorazio, A. J., J. K. Thomas, Q. A. Baker, and D. E. Ketchum. 2005. "An update to the Baker-Strehlow-Tang vapor cloud explosion prediction methodology flame speed table." *Process Safety Progress* no. 24 (1):59-65.
Raphael, J. M. 1962. "Prediction of temperature in rivers and reservoirs." *Journal of the Power Division, Proceedings of the American Society of Civil Engineers*.
Roberts, A. F. 1982. "Thermal-Radiation Hazards from Releases of LPG from Pressurized Storage." *Fire Safety Journal* no. 4 (3):197-212.

Schrage, J. 1991. "Vapor-Liquid-Equilibrium of the System H_2So_4-So_3 .1. Vapor-Pressure Measurements with a New Static Vapor-Pressure Apparatus." *Fluid Phase Equilibria* no. 68:229-245.
Shapiro, Ascher H. 1953. *The dynamics and thermodynamics of compressible fluid flow. Volume I*. New York: Wiley.
Sherman, M. 1980. *Air Infiltration in Buildings*, University of California, Berkeley.
Sherman, M., D. Wilson, and D. Keil. 1984. Variability in Residential Air Leakage. edited by Lawrence Berkeley Laboratory. Berkeley: Lawrence Berkeley Laboratory.
Sparrow, E. M., and R. D. Cess. 1978. *Radiation heat transfer*. Augmented ed, *Series in thermal and fluids engineering.* Washington: Hemisphere Pub. Corp.
Spicer, T., and J. Havens. 1989. User's Guide for the Degadis 2.1 Dense Gas Dispersion Model. Cincinnati: United States Environmental Protection Agency.
Thibodeaux, Louis J. 1979. *Chemodynamics, environmental movement of chemicals in air, water, and soil*. New York: Wiley.
Thomas, P.H. 1963. The size of flames from natural fires. Paper read at 9th International Combustion Symposium, at Pittsburgh.
Turner, D. Bruce. 1994. *Workbook of atmospheric dispersion estimates: an introduction to dispersion modeling*. 2nd ed. Boca Raton: Lewis Publishers.
Ullmann, Fritz. 2000. *Ullmann's encyclopedia of industrial chemistry*. 6th ed. New York: Wiley.
United States Office of the Federal Register. Code of federal regulations. Washington: Office of the Federal Register National Archives and Records Service General Services Administration.
United States. Environmental Protection Agency. 1987. *On-site meteorological program guidance for regulatory modeling applications*. Research Triangle Park, N.C.: U.S. Environmental Protection Agency Office of Air and Radiation Office of Air Quality Planning and Standards.
United States. Environmental Protection Agency. Chemical Emergency Preparedness and Prevention Office. 1999. Risk Management Program Guidance for Offsite Consequence Analysis. United States Environmental Protection Agency.
van Ulden, A. P. 1974. On the Spreading of Heavy Gas Released Near the Ground. In *First International Loss Prevention Symposium*. Delft, The Netherlands: Elsevier Scientific Publication.
van Ulden, A. P. 1983. A New Bulk for Dense Gas Dispersion: Two-Dimensional Spread in Still Air. In *I.U.T.A.M. Symposium on Atmospheric Dispersion of Heavy Gases and Small Particles*. Delft, The Netherlands.
Wagman, Donald D., and Frederick D. Rossini. 1965. *Selected values of chemical thermodynamic properties*. Washington: U.S. National Bureau of Standards.
Webber, D. M. 1991. "Source Terms." *Journal of Loss Prevention in the Process Industries* no. 4 (1):5-15.
Wiekema, B. J. 1984. "Vapor Cloud Explosions - an Analysis Based on Accidents .1." *Journal of Hazardous Materials* no. 8 (4):295-311.
Wilson, D. J. 1987. "Stay Indoors or evacuate to avoid exposure to toxic gas?" *Emergency Preparedness Digest* no. 14 (1):6.
Wilson, D. J. 1989. Personal Communication with William Lehr, 1989.
Wilson, D. J., Alberta. Pollution Control Division., and University of Alberta. Dept. of Mechanical Engineering. 1981. *Expansion and plume rise of gas jets from high pressure pipeline ruptures*. Edmonton: Pollution Control Division Alberta Environment.
Wilson, D. J., R. P. Angle, Alberta. Pollution Control Division., Alberta. Alberta Environment., and Alberta. Air Quality Control Branch. 1979. *The release and dispersion of gas from pipeline ruptures*. Edmonton: Air Quality Control Branch Pollution Control Division Environmental Protection Services.

Woodward, John Lowell. 1998. "Estimating the flammable mass of a vapor cloud." In. New York: Center for Chemical Process Safety of the American Institute of Chemical Engineers.
Zalosh, Robert, and Nathan Weyandt. 2005. "Hydrogen Fuel Tank Fire Exposure Burst Test." *S.A.E. Transactions* no. 114 (6):6.
Zeeuwen, J., and B. J. Wiekema. 1978. The measurement of relative reactivities of combustible gases. In *Conference on the Mechanisms of Explosions in Dispersed Energetic Materials*.

U.S. DEPARTMENT OF COMMERCE
Penny Pritzker,
Secretary

National Oceanic and Atmospheric Administration
Kathryn D. Sullivan, Ph.D.
Acting Under Secretary of Commerce for Oceans and Atmosphere, and Acting Administrator

National Ocean Service
Holly A. Bamford, Ph.D.
Assistant Administrator for Ocean Services and Coastal Zone Management